DEPARTMENT OF EXPERIMENTAL MEDICINE

PhD COURSE IN EXPERIMENTAL MEDICINE

Curriculum of Biochemistry

LANCL2 and ERRα Interaction and Functional Collaboration in Cardiomyocytes

Candidate: Zell-e-Humma

Tutor: Prof. Elena Zocchi

PhD Program Coordinator

Prof. Ernesto Fedele

Academic Year 2024-2025

XXXVIII Cycle

Borsa di dottorato cofinanziata con risorse dell'Unione europea-*NextGeneration EU*
Piano Nazionale di Ripresa e Resilienza Missione 4, componente 1 "*Potenziamento dell'offerta dei servizi di istruzione: dagli asili nido all'Università*"

ABSTRACT

Abscisic acid (ABA), a terpenoid phytohormone classically associated with plant stress responses, has emerged as an endogenous mammalian hormone with a conserved role in energy metabolism and immune regulation. In mammals, ABA modulates glucose homeostasis, mitochondrial function, and oxidative metabolism through its receptors, lanthionine synthetase C–like proteins LANCL1 and LANCL2. The orphan nuclear receptor estrogen-related receptor alpha (ERRα) is a master transcriptional regulator of mitochondrial biogenesis, oxidative phosphorylation, and metabolic flexibility in tissues with high energetic demand, including muscle and immune cells. Although both ABA/LANCL signaling and ERRα independently control cellular energy metabolism, their potential functional interplay has not been previously investigated. The objective of this doctoral research was to investigate the molecular and functional collaboration between the ABA/LANCL hormone–receptor system and ERRα signaling in cardiomyocytes and immune cells, with particular emphasis on nitric oxide (NO) and reactive oxygen species (ROS) metabolism, mitochondrial function, and transcriptional regulation. By integrating cellular, molecular, biochemical, and advanced imaging approaches, this study aimed to investigate the possible role of ERRα as a downstream effector of ABA/LANCL signaling and to explore the relevance of this axis in both metabolic and immune contexts.

Using rat embryonic H9c2 cardiomyocytes as a cell model, ABA stimulation and genetic modulation of LANCL1/2 expression were combined with ERRα silencing or overexpression. ROS production was quantified using H_2DCFDA and mitochondrial superoxide–specific MitoSOX™ assays, while NO signaling was evaluated through analysis of endothelial nitric oxide synthase (eNOS) expression. Transcriptional and protein-level changes were assessed by qPCR and Western blotting. Confocal microscopy and FRET–FLIM imaging were employed to investigate the subcellular localization and physical proximity of LANCL2 and ERRα, providing evidence of their spatial and functional association. In parallel, recombinant human ERRα was expressed and purified in *Escherichia coli* and reintroduced by plasmid transfection into LANCL2-overexpressing cardiomyocytes to validate causality in signaling responses. The results demonstrate that the ABA/LANCL1–2 system regulates NO and ROS metabolism in cardiomyocytes through an ERRα-dependent mechanism. ABA stimulation enhanced eNOS transcription and NO production, while concomitantly limiting excessive ROS generation, thereby promoting a metabolically efficient and redox-balanced phenotype. ERRα silencing significantly blunted these effects, establishing ERRα as a critical mediator of ABA/LANCL signaling. Confocal and FRET–FLIM analyses revealed co-localization and close molecular interaction between LANCL2 and ERRα in H9c2 supporting the existence of a functional

signaling hub linking membrane-associated ABA perception to nuclear transcriptional control of mitochondrial metabolism. To extend these findings to the immune system, LANCL2 expression was selectively silenced or increased in human $CD14^+$ monocytes and peripheral blood lymphocytes (PBLs). These experiments confirmed the feasibility of modulating the ABA/LANCL axis in immune cells and provided initial evidence that LANCL2 expression levels influence cellular metabolic and signaling competence, consistent with the established role of ERRα in immune cell activation and metabolic reprogramming. Together, these data suggest that the ABA/LANCL–ERRα axis represents a conserved metabolic signaling pathway operative in both cardiomyocytes and immune cells.

In conclusion, this thesis identifies ERRα as a novel downstream effector and functional partner of the ABA/LANCL hormone–receptor system, linking extracellular metabolic cues to transcriptional programs controlling mitochondrial function, redox homeostasis, and energy metabolism. These findings provide new mechanistic insight into insulin-independent, ABA-mediated metabolic regulation and highlight the ABA/LANCL–ERRα axis as a promising therapeutic target for metabolic disorders, cardiomyopathies, and immune-metabolic dysregulation. Future perspectives include in vivo validation of this signaling pathway, exploration of its role in blood glucose homeostatis, metabolic and inflammatory diseases, and the development of pharmacological or nutraceutical strategies aimed at selectively modulating ERRα activity downstream of ABA signaling.

Table of Contents

1. INTRODUCTION

The terpenoid plant hormone abscisic acid (ABA) controls a number of physiological functions in plants, including root elongation, seed dormancy and germination and fruit ripening. It also serves as a "stress" signal, allowing plants to react to various environmental cues such as light, water, and nutrient availability (Vishwakarma, 2017). Although ABA is generally associated with plants, more recent studies have shown that this hormone also plays an important role in several mammalian physiological functions, including blood glucose regulation (Spinelli, 2024 Nutrients). This introduction dwells on the physiological implications of the discovery of a new human hormone regulating glucose metabolism and the most recent advances regarding its signaling pathway, which provide the basis for this experimental thesis.

The high prevalence of diabetes worldwide and the forecasted further dramatic increase of the disease in developing countries contributes to raise the scientific interest in the potential therapeutic exploitation of ABA to improve glycemia control in hyperglycemic subjects. Diabetes is a chronic condition brought on by either insufficient insulin production by the pancreatic beta-cells or by insulin resistance. There is a general consensus among the scientific community regarding a causal role of excess visceral adipose tissue in the generation of insulin-resistance, due to the pro-inflammatory cytokines produced by white adipocytes. According to a 2024 WHO report, the percentage of persons aged 18 and over who had diabetes increased from 7% in 1990 to 14% in 2022. In 2022, over half (59%) of the subjects with diabetes who were 30 years of age or older did not take any medication for their condition. Diabetes was the direct cause of 1.6 million deaths in 2021, and 47% of all diabetes-related deaths occurred in people under 70. High blood glucose is responsible for about 11% of cardiovascular fatalities, and diabetes also contributed to another 530,000 deaths from kidney disease. Diabetes-related deaths have been rising since 2000. In contrast, between 2000 and 2019, the likelihood of dying from any of the three other major non-communicable illnesses (cancer, chronic respiratory conditions, or cardiovascular diseases) among people aged 30 to 70 years fell by 20% worldwide (https://vizhub.healthdata.org/gbd-results/). Individuals with high blood lipids, insulin resistance, excess body weight, and hypertension, all characteristics of the metabolic syndrome, are considered prediabetic or high-risk and are recommended to adhere to food and lifestyle guidelines, which are rarely followed. In light of the global trend towards an increase in the prevalence of overweight/obese subjects in both developed and developing countries, pharmacological or nutraceutical methods to induce the browning of WAT in humans are being actively investigated. This is due to the positive systemic metabolic effects observed in animal models of diabetes mellitus and fat liver disease upon increased energy expenditure.

In humans, insulin is the primary hormone that promotes tissue glucose uptake and metabolism. It is released by β-pancreatic cells in response to elevated glucose levels. This lowers glycemia and transforms glucose into storage forms, including glycogen and lipids (fatty acids, triglycerides, and VLDL), which the body can use when nutrients are scarce. Recent studies indicate that plasma ABA affects glycemic control and glucose metabolism in mammals. Numerous studies have demonstrated that ABA enhances oxidative glucose metabolism in muscle and adipose tissue, which results in the creation of metabolic energy and its dissipation as heat, and also stimulates myocyte and adipocyte glucose absorption in an insulin-independent way (Spinelli, 2024 Nutrients).

ABA promotes the transcription and plasma membrane translocation of the primary glucose transporters expressed in skeletal muscle, i.e. GLUT4 and GLUT1, as well as myocyte mitochondrial content and respiration, to stimulate glucose uptake in skeletal muscle at nanomolar doses. Through an insulin-independent mechanism, ABA lowers glycemia despite a decreased glycemia profile because it stimulates skeletal muscle glucose absorption, which happens both in vivo and ex vivo on the isolated muscle (Magnone, 2020). ABA is found in human plasma, and its concentration rises following a glucose load in normal subjects but not in T2D or gestational diabetic patients (Ameri, 2015). Interestingly, after childbirth, diabetes resolves and a normal plasma ABA rise resumes. These findings support the potential use of ABA to improve glycemic management (Bruzzone, FASEB J, 2012). The fact that ABA is a plant hormone enables the use of vegetal extracts as a natural supply of ABA, especially given the very low (nanomolar) blood levels required for efficacy. Vegetal extracts titrated in ABA naturally contain other chemicals; hence the observed effects cannot be attributed only to ABA. However, investigations indicated that the pure molecule and an identical amount incorporated in a vegetal extract were equally effective in lowering glycemia in mammals. Chronic low-dose ABA therapy (1 µg/Kg body weight) for four weeks improves glucose tolerance, muscle glycogen content, and physical resistance in mice (Magnone, 2020). The same dose of ABA, chronically administered to subjects with borderline values for prediabetes or who are prediabetic, significantly reduces all laboratory parameters used for diagnosing and monitoring (pre)diabetes: fasting blood glucose, glycated hemoglobin, HOMA-index, and response to an oral glucose tolerance test (OGTT) (Magnone, 2018).

The effect of ABA on skeletal muscle glucose metabolism is mediated by its receptors LANCL1 and LANCL2 (Spinelli, 2021). The mammalian LANCL proteins are a family composed of three members, showing significant sequence homology with bacterial enzymes producing the antimicrobial lanthionines, yet devoid of such enzymatic activity (He, 2017). LANCL1, a cytosolic protein, and LANCL2, which is instead membrane-bound via a myristoyl anchor, are both expressed in all human tissues, particularly in the brain, skeletal muscle and adipose tissue. Conversely, LANCL3 is expressed at very low levels and may be devoid of functional effects (https://www.proteinatlas.org/search/LANCL+). The ABA signaling pathway includes a membrane G protein complex receptor, ADP-ribosyl cyclase (ADPRC) phosphorylation and activation, overproduction of the universal calcium mobiliser cyclic ADP-ribose (cADPR), and a rise in intracellular calcium concentration $[Ca^{2+}]i$. This signaling pathway is conserved from lower Metazoa (Porifera, Hydrozoa) to mammals (Zocchi, 2003).

Estrogen-related receptors (ERR) are a family of transcription factors defined as “Orphan Nuclear Receptors” since their natural ligand is unknown, although they share a significant sequence homology with estrogen receptors. Since the discovery of the role of ERRs in the control of glucose energy metabolism and mitochondrial respiration in heart and skeletal muscle, the scientific interest in these proteins, particularly the alpha and gamma isoforms, has grown to include topics like development and differentiation, where metabolic reprogramming is fundamental. Since they definitely play an important role in musculoskeletal physiology, as demonstrated by loss- or gain-of-function experiments in rodents, ERRs are of great interest as potential therapeutic targets for the treatment of muscle atrophy, insulin resistance, diabetes and heart failure (Huss, 2015). The fact that ABA, via the LANCL receptors, also controls energy metabolism and mitochondrial function in muscle suggests that the ABA/LANCL hormone/receptors system may regulate ERR function.

The aim of this thesis was to investigate a possible molecular interplay between the ABA/LANCL1-2 system and ERRα signaling in the control of myocyte glucose oxidation and mitochondrial respiration. Identifying the ABA/LANCL hormone-receptors system as a trigger of ERR function would improve our understanding of the molecular mechanisms underlying muscle energy metabolism and could provide new means for therapeutic intervention in diseases such as diabetes, muscle atrophy and heart failure.

2. LITERATURE REVIEW

2.1. Evolution of ABA as an Endogenous Hormone

More than 20 years after its discovery in plants (Addicott, 1968), ABA was also described as an endogenous hormone in Metazoa. Le Page-Degivry et al. showed in 1986 that ABA was present in the brains of mice given a synthetic diet devoid of ABA in significantly larger proportions than in animals fed a standard (ABA-containing) chow (Le Page-Degivry, 1986). Fifteen years later, investigations on early Metazoa (sponges and hydroids) revealed a cross-kingdom conserved role for ABA as an endogenous stress hormone, paving the way for research on more complex animals (Zocchi, 2001; Puce, 2004). In 2012, researchers discovered that plasma ABA levels rise in healthy adults after glucose intake, reaching amounts in the low nanomolar range, providing strong evidence that ABA is an endogenous hormone in humans. Finally, the identification of the LANCL proteins as mammalian ABA receptors, LANCL2 in 2011 and LANCL1 in 2021, shed light on ABA functions and signaling pathways through the study of gain- and loss-of-function in overexpressing vs. silenced cells, as well as in KO mice (Spinelli, 2023). Significant milestones in the identification of ABA as a mammalian hormone are summarized in Fig 1.

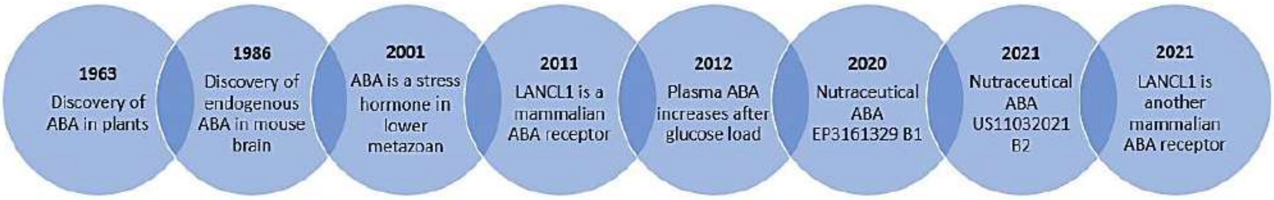

Figure 1: Milestones in the identification of ABA as an animal hormone. It took more than 20 years from the discovery of ABA in plants to its initial identification as an endogenous molecule in the mammalian brain. Later research on ABA function as a stress hormone in early Metazoa (marine sponges and hydroids) identified ABA as an endogenous mammalian hormone (2012) with LANCL1 and LANCL2 as its receptors. Following in vivo research on humans and rodents, patent applications for the use of ABA as a nutraceutical to enhance glucose tolerance and metabolism were filed and granted in the US in 2021 and the EU in 2020.

2.2. ABA Receptors and Signaling Pathway in Blood Glucose Regulation

2.2.1. LANCL Proteins

The lanthionine synthetase C-like (LANCL) protein family is structurally similar to bacterial lanthionine synthetase C proteins, which are responsible for the production of lantibiotics such as nisin. These lantibiotics are widely used to prevent bacterial development in food products (Shin, 2016). However, because lantibiotics do not originate in animals, mammalian LANCL proteins must function differently from bacterial LanC proteins (He, 2017). The human genome contains three LANCL genes: LANCL1, LANCL2, and LANCL3, which are found on chromosomes 2, 7, and X, respectively. While LANCL1 and LANCL2 are found in almost every tissue, particularly in skeletal muscles, immune cells, and the brain (see https://www.proteinatlas.org/search/LANCL, accessed on October 20, 2024), both as transcripts and proteins, LANCL3 transcription is extremely low, suggesting that it is a pseudogene.

LANCL2 was shown to be necessary for ABA binding and signaling in four distinct cell types from two mammalian species (rat microglia and insulinoma cells, and human granulocytes and HeLa cells): (i) in human granulocytes, LANCL2 silencing inhibited the ABA-induced rise in cytosolic free calcium [Ca^{2+}]cyt and cAMP as well as the ABA-triggered functional response in these cells (ii) LANCL2 overexpression, on the other hand, enhanced the ABA-induced [Ca^{2+}]cyt increase in granulocytes and enabled ABA responsiveness in $CD38^{+}$ HeLa cells, as evidenced by elevated levels of [Ca^{2+}]cyt and cAMP; and lastly, (iii) in two distinct rat insulinoma cell lines, LANCL2 silencing eliminated the ABA-induced increase in [Ca^{2+}]cyt and cAMP and functional responses (Sturla, 2009). Direct ABA binding to both LANCL 1 and LANCL2 was demonstrated by in vitro binding assays using the recombinant human proteins (Sturla, 2011; Spinelli, 2021).

Human granulocytes and rat cardiomyocytes have been studied in detail in relation to the ABA signaling pathway in mammalian cells. Adenylate cyclase (AC) and phospholipase C are both activated in granulocytes by LANCL2, which leads to an increase in [Ca^{2+}]cyt that is mediated via IP3 and CD38-produced cADPR (Bruzzone, 2007). This ABA signaling pathway, summarized in Fig 2, which involves AC, cAMP, the protein kinase A (PKA)-dependent activation of the ADP-ribosyl cyclase CD38, cADPR overproduction, and [Ca^{2+}]cyt rise, has been conserved from sponges and hydroids to human innate immune cells. This suggests that it evolved early as a mechanism to enable adaptation to environmental challenges by eliciting an intracellular Ca^{2+} wave, which is arguably the most ancient and conserved trigger of cell functional responses. It has recently been discovered that AMPK is activated by the ABA/LANCL hormone/receptors system in rat cardiomyocytes and human adipocytes (Spinelli, 2023). AMPK is an evolutionary conserved sensor of cell and whole organism energy status which activates mitochondrial biogenesis, oxidative phosphorylation, oxygen consumption and antioxidant protection, along with glucose transport and oxidative metabolism. As a master regulator of cell energy metabolism, AMPK and the signaling pathways that control its activation are being intensely investigated as potential pharmacologic targets for several diseases, including obesity, diabetes and cancer. Downstream of the activation of AMPK, PGC-1α and ERRα trigger a complex, multi-gene transcriptional response which increases mitochondrial generation and oxidative function (Malik, 2023).

The fact that the ABA/LANCL system is a trigger of AMPK activation in cardiomyocytes suggests that ERRα may be part of the signaling cascade of ABA.

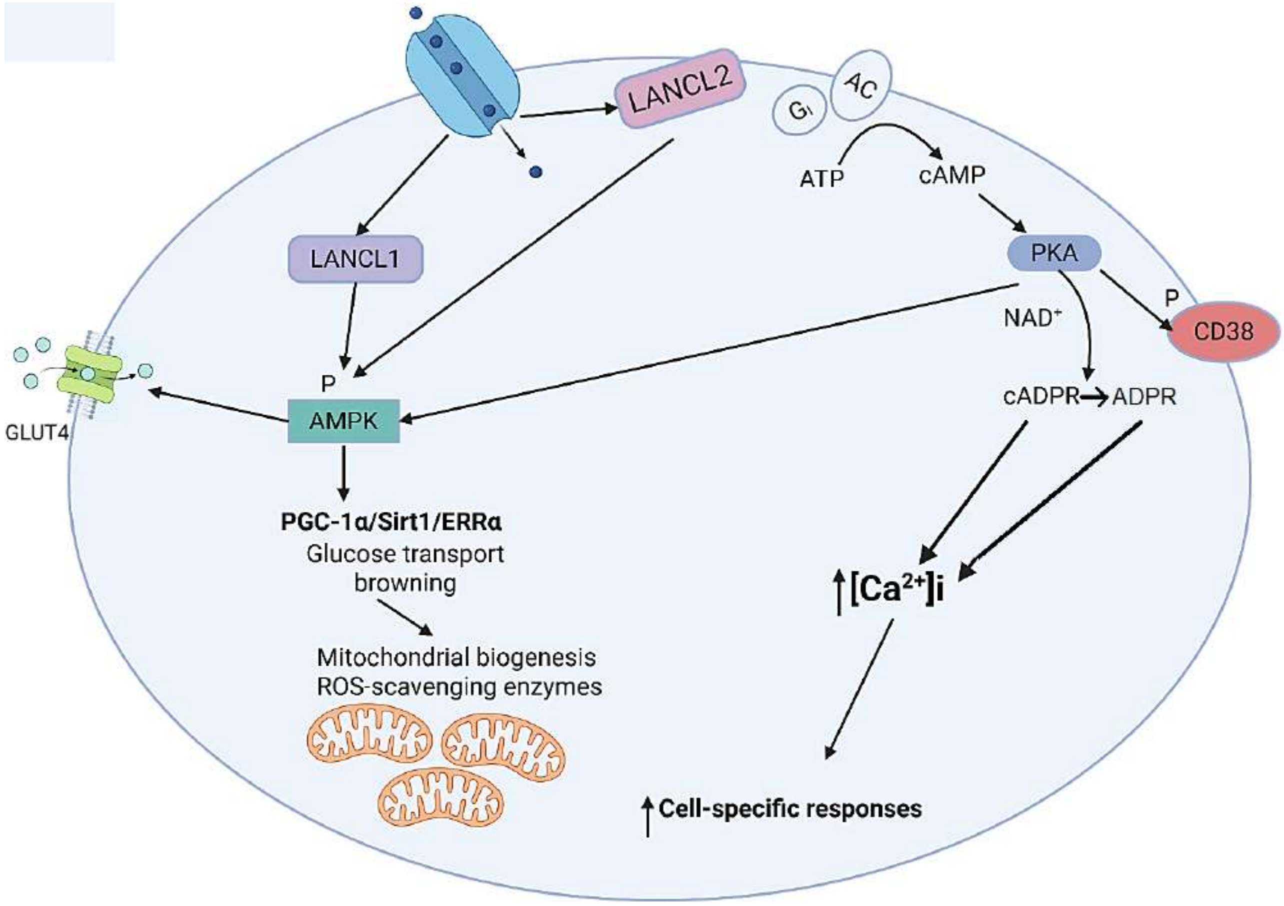

Figure 2: Main functional effects of ABA on cellular metabolism and ABA-activated signaling pathways. The most common form of ABA at neutral pH, deprotonated ABA, attaches to its receptors, membrane-anchored LANCL2 and cytosolic LANCL1, after passing through the plasma membrane via an anion transporter. Both receptors have the ability to activate the PGC-1α/sirtuin 1/ERRα axis and AMP-dependent kinase (AMPK), which in turn activates transcriptional programs that regulate antioxidant defenses, mitochondrial activity, and glucose uptake. Additionally, downstream of LANCL2, protein kinase A (PKA) is activated, which phosphorylates and activates the ADP-ribosyl cyclase CD38. This results in the production of cyclic ADP-ribose (cADPR) and ADP-ribose, both of which contribute to the creation of a cytosolic Ca^{2+} wave through extracellular Ca^{2+} entry (mediated by ADPR-gated plasmamembrane channels) and intracellular Ca^{2+} release from ryanodine-sensitive stores (operated by cADPR).

2.2.2. Role of LANCL1/2 Proteins in Blood Glucose Homeostasis

LANCL2 silencing reduces, but does not completely eliminate, the effect of ABA in muscle and adipose cells, indicating that additional receptors may play a part in the hormone's metabolic activity (Sturla, 2017). Experiments performed on the LANCL2 KO mouse provided a more direct indication that additional receptors were involved in mediating the metabolic activities of ABA. Although LANCL2 KO mice do have a lower glucose tolerance than their wild-type siblings, they nonetheless respond to exogenous ABA (1 µg/kg body weight (BW)/day), which dramatically lowers the AUC of glycemia following a glucose load to levels comparable to those of wild-type animals (Spinelli, 2021). These findings suggest that LANCL2 deficiency impairs glucose tolerance, but they also show that another receptor can act as a stand-in for LANCL2 in stimulating the transport of glucose through muscle and adipose tissue, albeit at higher ABA concentrations than those attained by the endogenous hormone. In fact, plasma ABA (ABAp) rises 10–50 times higher than endogenous levels in humans when ABA is consumed at a dose of 1 µg/kg BW plasma (Magnone, 2015). It appears that a lower affinity receptor may not be activated by decreasing endogenous ABA levels, but it can be recruited by the increase in ABAp brought about by exogenous ABA supplementation. Since LANCL1 and LANCL2 have a significant sequence identity (54.2%), and they share an intracellular localization (LANCL2 is membrane-associated but not transmembrane and LANCL1 is cytosolic), and tissue expression pattern, LANCL1 is an obvious candidate for this role. Interestingly, LANCL1 is spontaneously overexpressed in cells or animals when LANCL2 is silenced or genetically removed. Similarly, in L6 muscle cells, LANCL2 expression is markedly elevated when LANCL1 is silenced. The functional redundancy of the ABA receptors and their physiological significance in mammals can be inferred from these findings.

As observed in vitro, in rat myoblasts, and in vivo, in murine skeletal muscle, both LANCL1 and LANCL2 activate the same signaling pathway (the AMPK/PGC-1α/Sirt1 axis), leading to similar transcriptional and functional responses: increased glucose uptake and metabolism, mitochondrial respiration, and uncoupling (Spinelli, 2021).

2.2.3. AMPK Activation Downstream of LANCL1/2

Experiments conducted on L6 myoblasts in vitro and on murine skeletal muscle in vivo show that ABA promotes muscle glucose transport in the absence of insulin and that this action is mediated by AMPK activation. In L6 cells and mouse muscle, ABA does in fact raise AMPK phosphorylation on Thr172 and induces increased AMPK transcription. When L6 myoblasts were pre-incubated with AZD5363, a pan-Akt competitive inhibitor, the pAMPK levels in ABA-treated cells were considerably higher than in untreated cells. This suggests that Akt has an inhibitory influence on ABA-induced AMPK activation. In fact, AMPK phosphorylation on Thr172 by LKB1 is inhibited when Akt is activated by phosphorylation on both Thr308 and Ser473. In the fed state, insulin promotes double phosphorylation (on Ser473 and Thr308) and maximal activation of Akt, which initiates cell energy storage, primarily through the synthesis of glycogen and triglycerides, while simultaneously blocking AMPK phosphorylation and activation by LKB1 (Magnone, 2020). On the other hand, AMPK activation takes place when there is less cell energy available and promotes mitochondrial and metabolic processes acting to restore energy balance. Both ABA- (through AMPK) and insulin- (through Akt) induced signaling share the characteristic of stimulating cell glucose absorption, which permits energy synthesis and storage, respectively. During an oral glucose load, ABA-treated rats' glucose absorption, as measured by dynamic micro-PET in skeletal muscle, doubles in comparison to untreated rats. Since skeletal muscle makes up a large portion of body weight (around 45%) in rodents, the higher muscle glucose absorption is probably what causes the faster blood glucose clearance seen in ABA-treated mice as opposed to control mice (Magnone, 2020).

2.2.4. ABA Signaling in Skeletal Muscle

The AMPK/PGC-1α/Sirt1 axis controls the signaling pathway that ABA activates in skeletal muscle. This leads to increased gene transcription and protein overexpression of the glucose transporters GLUT1 and GLUT4, the NAD-synthesizing enzyme Nampt, RabGAPTBC1D1, the muscle-specific mitochondrial uncoupling proteins UCP-3 and sarcolipin, as well as an increase in mitochondrial DNA content (Spinelli, 2021). Muscle glucose uptake and energy metabolism are enhanced by ABA's transcriptional and translational actions, which raise muscle glucose consumption. LANCL2 KO animals with streptozotocin (STZ)-induced diabetes do respond to ABA similarly to wild-type mice, if not better. This could be explained by the higher muscle expression of LANCL1 in LANCL2KO mice as compared to wild-type siblings (Magnone, 2022). Furthermore, LANCL2 KO animals have elevated levels of AMPK, PGC-1α, GLUT1/4, Nampt, and UCP-3 expression, as well as a higher skeletal muscle mitochondrial DNA content than wild-type mice. These levels further rise following long-term ABA administration. In the skeletal muscle of ABA-treated wild-type and LANCL2 KO mice, we found a substantial increase in the transcription of important glycolytic enzymes (GaPDH, PFK1) and PDH in comparison to untreated controls. This is anticipated to promote oxidative muscle glucose consumption. Remarkably, when compared to their wild-type counterparts, LANCL2 KO female mice, with LANCL1-overexpressing muscles, gained far less body weight when given a high-glucose diet for three months. These results imply that the ABA/LANCL system-regulated increased oxygen demand and muscle and adipocyte mitochondrial uncoupling may impact total body energy consumption. LANCL2 KO mice had a significantly lower mean glycemia than wild-type mice at the end of a similar regimen that involved ABA pretreatment followed by low-dose streptozotocin, to induce diabetes. The overexpression of LANCL1, which can bind ABA and activate its signaling pathway in place of LANCL2, is responsible for these effects. Finally, long-term ABA administration may enhance muscle sensitivity to endogenous and exogenous insulin, as evidenced by the enhanced transcription of the insulin receptor mRNA in the skeletal muscle of mice receiving chronic ABA treatment. Interestingly, ABA-treated mice showed a significantly improved physical performance on a running wheel, compared with untreated controls, likely as a result of the increased muscle glucose uptake and mitochondrial oxidation (Magnone, 2020).

2.3. Insulin and ABA have Non-Overlapping Functions in Energy Metabolism

The aforementioned findings suggest that insulin and ABA have distinct roles in muscle and adipocyte metabolism. Akt is phosphorylated by insulin, which inhibits AMPK, changes the metabolic program from the starving to the fed state, activates glucose transport and metabolism, and stores surplus glucose abundance through the synthesis of proteins, lipids, and glycogen (Fig 3). Instead, ABA causes AMPK to become phosphorylated, which initiates the metabolic reaction to low glucose availability and/or hunger (Spinelli, 2023). This reaction involves activating mitochondrial biogenesis, respiration, oxphos uncoupling (and consequent thermogenesis), and glucose transport and oxidation for energy production. Together, this background enables us to recognize the ABA/LANCL system as a novel regulator of mitochondrial energy generation and glycemia homeostasis, as well as a potential new therapeutic tool in pathological states like (cardio)myopathies, diabetes mellitus, and tissue hypoxia.

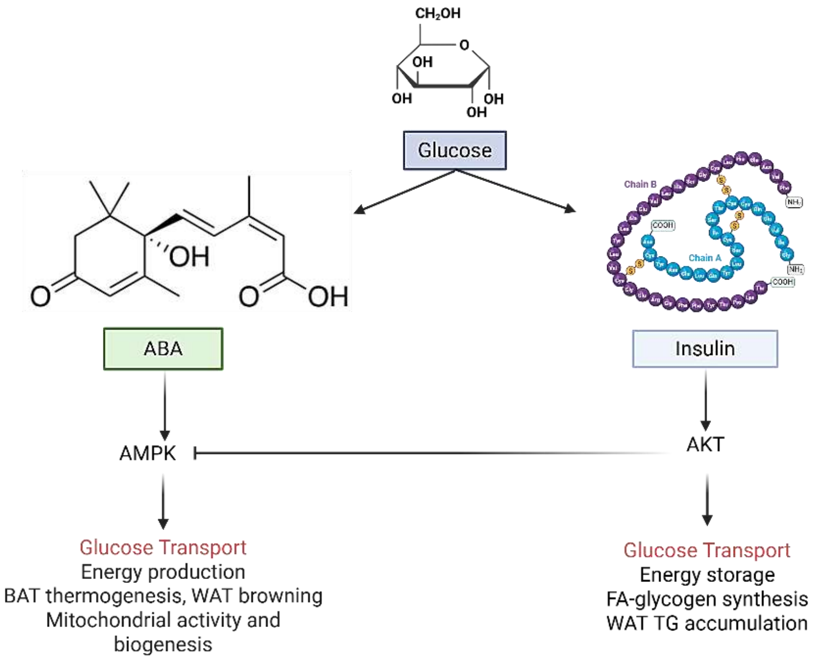

Figure 3: Insulin and ABA have non-overlapping roles in muscle and adipose tissue. Insulin and ABA both stimulate muscle and adipose tissue to transport and utilize glucose. Insulin promotes the transformation of metabolic energy into storage forms, including muscle glycogen, fatty acids, and white adipocyte triglycerides, through the action of Akt. Conversely, ABA activates AMPK, which is inhibited by Akt (blunted red line), and stimulates mitochondrial energy generation and biogenesis, also resulting in increased heat dissipation by uncoupling proteins. FA stands for fatty acids; TG for triglycerides; BAT for brown adipose tissue; and WAT for white adipose tissue.

2.4. Plasma ABA in Glucose Homeostasis

In animals, glucose/nutrient-sensing cells release two peptide hormones: intestinal endocrine cells release glucagon-like peptide 1 (GLP-1) and pancreatic islet β-cells release insulin. Among other actions, GLP-1 helps to promote the release of insulin and prevents the pancreatic α-cells from secreting glucagon, the main hormone that is triggered by low blood glucose. In healthy individuals, ABAp also rises following an oral glucose load; however, this is not the case in individuals with type 2 diabetes (T2D) or gestational diabetes mellitus (GDM). Normal ABAp is restored together with the resolution of the postpartum diabetic state in GDM, indicating a crucial function for ABAp in maintaining normal glucose tolerance and a potential new ABA-centered pathogenetic pathway that could be responsible for the diabetic condition. Since insulin resistance or insufficiency lower glucose tolerance in diabetes mellitus, finding a second hormone that can promote muscle glucose uptake in addition to insulin would have significant therapeutic implications (Ameri, 2015). In patients with type 1 diabetes (T1D), ABAp is either undetectable or very low along with insulin, indicating that β-cells are the primary source of endogenous ABA in humans. As a result, the death of β-cells in T1D significantly lowers the availability of both glycemic-regulating hormones, of which only one is currently replaced by therapy. Because insulin and ABA activate different metabolic processes, taking supplements of one hormone will not correct the lost function of the other one.

In rats and healthy humans exposed to a glucose load, low-dose oral ABA does, in fact, lower glycemia and insulinemia. The glycemia-lowering effect of low-dose ABA in vivo reduces the activation of β-cells by hyperglycemia, which in turn inhibits insulin release. ABA has a very high therapeutic index because, unlike insulin, it does not cause hypoglycemia, even at a dose 100,000 times higher than the one that is effective in lowering glycemia (100 mg/Kg body weight vs. 1 µg/Kg body weight). Because there is no risk of hypoglycemia from excessive dosage, ABA differs significantly from both insulin and oral hypoglycemic medications.

Interestingly, the LANCL1 gene is found inside the Insulin-dependent diabetes (Idd) 5.3 locus, which confers resistance to T1D in NOD mice (Hunter, 2007). LANCL1 is also one of the putative genes responsible for the observed complicated phenotype of decreased neuronal function caused by a microdeletion in the chromosomal region 2q34 (Westphal, 2018).

ABA can be taken orally, is easily absorbed since the protonated molecule is membrane permeant in the acidic stomach environment, and has a high plasma concentration for several hours after consumption, most likely as a result of its binding to plasma proteins, which reduces renal clearance (Magnone, 2015).

2.5. Role of ABA in Innate Immune Cells.

2.5.1. Granulocytes

As they represent the first line of defense in innate immunity, granulocytes are quickly drawn to infection or injury sites in response to chemotactic cues, like host-derived signals or pathogen-associated molecular patterns (PAMPs). After they arrive, they phagocytose pathogens and generate reactive oxygen and nitrogen species (ROS and RNS), including nitric oxide (NO), which aid in the destruction of microorganisms and the reduction of inflammation. The $[Ca^{2+}]i$ rise brought on by cADPR is necessary for these granulocyte activities (Bruzzone, 2007). In human granulocytes, ABA promotes a number of physiological processes, such as phagocytosis, the generation of ROS and NO, and chemotaxis. At 50 nM and 20 µM, ABA considerably and noticeably enhanced phagocytosis, respectively. In comparison to the controls, ABA at 20 µM caused a 6-fold rise in ROS, a 1.83- to 9.42-fold (median 3.55-fold) increase in NO generation, and a minor but steady increase in granulocyte chemokinesis (untargeted cell movement). Cell migration increased significantly at 50 nM and reached its maximum at 20 µM as a result of ABA's induction of a concentration-dependent chemotactic response. ABA-methylamide and (±)-trans (racemic mixture), trans ABA, on the other hand, had no impact (Bruzzone, 2007). Granulocytes exhibited increased ABA production and secretion upon fMLP stimulation, whereas NDGA (nordihydroguaiaretic acid)-induced ABA biosynthesis inhibition markedly decreased intracellular ABA levels and extracellular release, indicating that de novo synthesis is necessary for ABA secretion in these cells. The addition of ABA can restore the 80% reduction in ROS generation that was achieved by removing the elevated ABA from the supernatant of particle-stimulated granulocytes using an anti-ABA mAB. These findings show that ABA works as a pro-inflammatory endogenous autocrine cytokine that can stimulate granulocyte activity (Bruzzone, 2007).

2.5.2. Monocytes

As was previously mentioned, monocytes are essential for both innate and adaptive immunity because of their capacity to present antigens, phagocytose pathogens, and secrete a range of growth factors and cytokines. When human monocytes isolated from peripheral blood mononuclear cells (PBMCs) were exposed to ABA at 1 to 100 µM, NF-κB was activated, which in turn caused an increase in the production of prostaglandin E2 (PGE2) and cyclooxygenase-2 (COX2), as well as a greater release of MCP-1 and metalloprotease-9 (MMP-9). Reports state that all of these processes are involved in atherogenesis. ABA may therefore actively aid in the development and advancement of atherosclerotic lesions by triggering NF-κB activation and the expression of important pro-inflammatory mediators in monocytes (Magnone, 2009). When exposed to inflammatory stimuli, cytosolic NF-κB translocates to the nucleus following Ca^{2+}- and PKC-dependent phosphorylation of the NF-κB inhibitor, IκB. Incubation of monocytes with ABA for 30 minutes resulted in a dose-dependent increase in NF-κB nuclear translocation, with the highest value being a 2.17-fold increase when compared to the controls.

The expression of NF-κB-controlled genes, COX-2, MCP-1, and MMP-9 (which catalyses the proteolytic cleavage of the extracellular matrix and promotes monocyte extravasation and Vascular Smooth Muscle Cells (VSMC) migration through the blood vessel wall), was elevated. COX-2 expression was increased 1.3-, 1.4- and 1.6-fold in the cells treated for 6 h with 0.1, 1.0, and 10 µM ABA, respectively. The release of MCP-1 and MMP-9 peaked with 2.3-fold and 1.8-fold increases, respectively, when monocytes were incubated with 10 µM ABA for 6 h. The synthesis of prostaglandin E2 (PGE2) was increased 1.8-fold (maximum), compared to the control, by concentrations of ABA as low as 0.1 µM. These data indicate that ABA induces overexpression of NF-κB-controlled atherosclerosis-related proteins in human monocytes (Magnone 2009).

Human monocytes have been shown to release ABA, which can activate VSMC proliferation and attract and activate other monocytes, resulting in cell responses conducive to repair of the internal blood vessel lining. The ABA concentration measured in biopsies taken from human atherosclerotic plaques were 10-fold higher than in non-atheromatous vascular tissue, or 0.02 pmol/mg wet weight ABA, which is equivalent to 20 nM, a concentration within the range of concentrations (10–100 nM) that induce functional effects in both monocytes and VSMC. MCP-1 is believed to be the primary chemoattractant for monocytes to the atherosclerotic plaques, and it also stimulates VSMC proliferation. Nanomolar concentrations of ABA stimulate MCP-1 release from monocytes, and MCP-1, in turn, stimulates ABA release from monocytes (Magnone, 2009).

2.6. Localization of LANCL Protein

LANCL2 is not a transmembrane protein, as could be predicted by its sequence in silico, but it is attached to the inner side of the plasmamembrane, as it can be extracted without the need for detergents (Vigliarolo, 2015), either by mild chemical treatments or by inhibiting its post-translational N-terminal myristoylation (Fresia, 2016). Furthermore, the LANCL2-GFP fusion protein that is not myristoylated has been discovered to be restricted to the nucleus. This finding suggests that ABA, its hormone ligand, might have an impact on LANCL2 trafficking across membranes and the nucleus. Recent research has demonstrated that the human anion exchanger AE1 mediates ABA transport across the plasma membrane, which helps to reconcile the non-transmembrane localization of

LANCL2 with its hormone receptor activity (Vigliarolo, 2015). By means of several techniques, including site-directed mutagenesis, confocal fluorescence microscopy, fluorescence recovery after photobleaching (FRAP), and photoactivation techniques, researchers examined the peculiar characteristics of LANCL2 among G protein-coupled animal hormone receptors (GPCR). Researchers investigated the location, intracellular mobility, and interaction of LANCL2 with Gi in the presence of ABA.

2.6.1. The Function of N-Terminal yrMistoylation in the Subcellular Localization of LANCL2

Several lines of evidence obtained from saturation binding, scintillation proximity assays, dot blot experiments and affinity chromatography indicate that LANCL2 binds ABA (Sturla, 2011). More recent results, employing equilibrium binding assays ([^{3}H]-ABA saturation binding and surface plasmon resonance analysis) on the recombinant human protein, and computational studies, indicate presence of multiple ABA-binding sites: one with high-affinity (in the low nanomolar range) and two with lower affinity (in the micromolar range). Site-directed mutagenesis (single mutant R118I, triple mutants R118I/R22I/K362I and R118I/S41A/E46I) and equilibrium binding experiments on the mutated LANCL2 proteins identified a high-affinity ABA-binding site involving R118, with a KD of 2.6 nM ± 1.2 nM, as determined by surface plasmon resonance (Cichero, 2018).

A comparison of the three LANCL genes reveals that Met 19 of LANCL2 corresponds to the start methionine of the highly similar cytosolic proteins LANCL1 and LANCL3. Thus, transcription of a "shortened" version of LANCL2, beginning at Met 19, produces a protein that lacks the myristoylated glycine and the 18-aminoacid N-terminal stretch that distinguishes LANCL2 from LANCL1. In order to investigate the role of the N-terminal peptide, which allows LANCL2 myristoylation and plsmamemrbane anchoring, in the subcellular trafficking of the protein, different types of LANCL2 protein were transiently transfected into HeLa and HEK cells: LANCL2 fused to EGFP (LANCL2-GFP), untagged LANCL2, G2A mutagenized LANCL2 (LANCL2-G2A), G2A mutagenized LANCL2 coupled to EGFP (LANCL2-G2A-GFP), and short LANCL2 linked to EGFP (LANCL2sh-GFP). In HeLa cells, LANCL2-GFP co-localized with a myristoylated plasma membrane marker, which was produced by expressing the red fluorescent protein fused to the myristoylation/palmitoylation sequence from Lck tyrosine kinase. Untagged wild-type LANCL2 was detected using a specific monoclonal antibody, demonstrating that LANCL2 localizes to the plasma membrane even in the absence of tags. To test the effect of the de-myristoylation on LANCL2 localization, HEK cells transiently overexpressing LANCL2-GFP were treated with or without 1 mM HMA. After 24 hours, the majority of the protein in the HMA-treated cells was found in the nucleus, consistent with prior findings, but not in the nucleoli, contrary to earlier observations. HeLa expressing untagged LANCL2 treated with HMA and stained with the anti-LANCL2 mAb, as well as cells expressing either mutagenized non-myristoylatable LANCL2-G2A-GFP or untagged LANCL2-G2A, demonstrated the nuclear localization of non-myristoylated LANCL2. Thus, in both HeLa and HEK cells, no discernible localization differences were observed between different GFP-tagged and untagged LANLC2 recombinant forms. In particular, both the GFP-tagged and untagged proteins were found in the nucleus when the myristoyl anchor was lost as a result of chemical (HMA) or genetic suppression of myristoylation, whereas full length myristoylated LANCL2 was found in the cytoplasm and the plasma membrane. These results suggested to explore the presence of nuclear localization signals in LANCL2. With a comparable score of 3.6/10, the software NLS predictor cNLS Mapper found two putative NLS sequences in the N-terminal region of LANCL2: a bipartite NLS (K7-G37) and a monopartite NLS (T4-H12). In fact, the shortened form of LANCL2-G2A-GFP, which is devoid of the N-terminal peptide that contains the NLS, exhibited a uniform distribution throughout the cell, while LANCL2-G2A-GFP primarily localized inside the nucleus (Fresia, 2016).

2.6.2. Impact of LANCL2 Localization on its Function

Researchers looked into how ABA perception and signaling are impacted by the myristoylation-dependent membrane localization of LANCL2. When ABA binds to LANCL2, the β γ subunit complex that is released from an active Gi-protein stimulates AC (Sturla et al., 2009). FRET experiments were performed to ascertain whether LANCL2 directly interacted with the α subunit of a Gi-protein by labelling the α subunit of a chimeric Gi protein, which is known to be activated by LANCL, with an acceptor fluorophore (TagRFP, Gi-RFP), and LANCL2 with a donor fluorophore (EGFP) at the C-terminus (LANCL2-GFP). The EGFP-tagged soluble short form of LANCL2, LANCL2sh-GFP, was used as a negative, nonmembrane-associated control. HeLa cells co-transfected with LANCL2-GFP and Gi-RFP produced a detectable FRET signal, suggesting that the acceptor (TagRFP) and donor (EGFP) were close enough to allow for resonance energy transfer. Remarkably, FRET between LANCL2 and the Gi α subunit was detected in intracellular regions as well as on the plasma membrane (which was identified by the strong signal at the cell border and examined using manually drawn ROIs). The average apparent FRET efficiency determined for the LANCL2-Gi couple in plasma membrane ROIs (20 ± 7%) was comparable to the FRET determined in whole-cell regions (20 ± 5%; n = 40 cells in five distinct transfection experiments). In contrast, co-transfection of the Gi-RFP with soluble LANCL2sh-GFP resulted in the loss of the association (FRET efficiency 1 ± 2%). Based on these findings, it was concluded that a membrane-associated, myristoylated LANCL2 is necessary for the interaction with the α subunit of the chimeric Gi-protein (Fresia, 2016).

Next, the ABA-binding capacity of the truncated short version of LANCL2 fused with GST (LANCL2sh-gst) and the full-length recombinant LANCL2, equally fused with GST (LANCL2-gst) were compared. Both proteins were cleaved from their GST tag in the absence of DTT, which resulted in a higher ABA binding affinity than previously observed (Sturla, 2011). In fact, the presence of several cysteines in the LANCL2 sequence suggests presence of disulphur bonds, which might be sensitive to excess DTT. Both proteins exhibited identical affinities for selective and saturable [^{3}H]-ABA binding (Kd values for LANCL2 and LANCL2sh were 8.9 ± 1 μ M and 10.6 ± 1.4 μ M, respectively). Therefore, ABA binding does not require the amino acid N-terminal stretch of LANCL2, which contains the myristoylation site. Lastly, by monitoring the rise in intracellular cAMP concentration ([cAMP]i) in transfected HeLa cells after ABA was added, the capacity of various LANCL2 forms to initiate the ABA-signaling pathway was investigated (Fresia, 2016). The [cAMP]i was measured 30 seconds after HeLa cells transfected with untagged LANCL2, LANCL2-GFP, or the untagged mutagenized LANCL2 (LANCL2-G2A) were treated with 5 μ M ABA. HeLa cells that overexpressed untagged LANCL2 (165 ± 19% over baseline, unstimulated values, $p < 0.02$) or LANCL2-GFP (170 ± 21%, $p < 0.02$) showed an increase in [cAMP]i. However, in cells transfected with the non-myristoylatable LANCL2-G2A, the [cAMP]i was not significantly altered in comparison to basal values (94 ± 17%, $p = 0.6$). Accordingly, the ABA-triggered activation of adenylate cyclase requires both LANCL2 myristoylation and a functional connection between LANCL2 and the chimeric Gi α subunit, both of which are satisfied at the plasma membrane and internal membranes in the cytoplasm. On the other hand, binding of ABA does not require LANCL2 to associate with the plasma membrane. This finding implies that LANCL2 may be able to bind ABA and initiate other, cAMP-independent signaling pathways if it is unmyristoylated and hence readily diffusible.

2.7. Estrogen Related Receptors: Protein Family and Tissue Expression

Estrogen-related receptors (ERRs) are evolutionary conserved nuclear receptors (NR), present since the earliest and simplest Metazoa, deriving their name from their sequence similarity with estrogen receptors, another group of NR. NR are a protein super-family with highly conserved structural features, no doubt a testament to their having evolved through numerous gene duplications. ERRs are enlisted among the so-called “orphan receptors” in that their cognate ligand is not known; however, their mechanism of action as controllers of gene expression occurs through their binding, together with other co-regulatory proteins, to specific DNA sequences known as Estrogen Related Receptor Elements (ERREs). ERRs control transcription of genes involved in generation and control of metabolic energy, mitochondrial function and biogenesis, tissue repair and response to hypoxia. Thus, being placed at the crossroads between energetics and homeostasis, ERRs (in association with coregulatory molecules) can facilitate cell and tissue repair and adaptation to stressful environmental conditions.

Estrogen-related receptors α (ERRα) and β (ERRβ) were discovered in 1988 (Giguère, 2002) and ten years later a third family member ERRγ (ERRγ) was discovered. Significant sequence similarity exists between the ERR family (Fig 4) and the ligand-binding domain (LBD) and DNA binding domain (DBD) of the estrogen receptor ERα. Despite this similarity, ERRs are categorized as orphan nuclear receptors since they are unable to bind estrogen or its derivatives (Huss, 2015). There are no known splice variants for ERRα in human tissues, three for ERRβ, and two for ERRγ. The proteome's functional diversity is greatly enhanced by these splice variations. However, the paucity of research on these splice variants hinders a thorough understanding of their functional roles. The six conserved sections (A/B, C, D, and E/F domains) that make up the molecular architecture of ERRs are quite similar to those of other steroid nuclear receptors. The general structure of the three ERR proteins is depicted in Fig. 4.

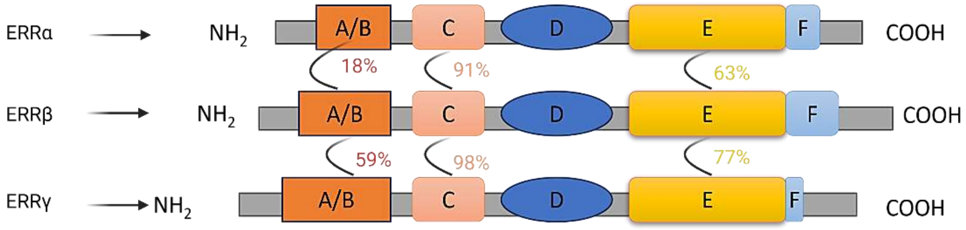

Figure 4. The structure of the three estrogen-related receptors (ERRs) proteins. A/B, C, D, and E/F are the six conserved domains that make up ERRs. The sequence identity of the corresponding domain between distinct receptors is shown by the number between the two.

The N-terminal region is characterized by ligand-independent transcriptional activation, also referred to as the A/B domain or activation function-1. ERRs' conserved motifs in their A/B domains can be controlled by post-translational changes such as phosphorylation and SUMOylation (Vu, 2007). Two extremely conserved zinc finger motifs that can attach to the ERR response element—a particular DNA sequence (TCAAGGTCA)—are found in the central C domain, also known as the DNA-binding domain. With nearly identical C domains, multiple isoforms of ERRs can target the same gene by forming monomers, homodimers, or heterodimers with other isoforms. The D domain connects the C and E sections and functions as a flexible hinge region, giving the protein flexibility when binding DNA. The ligand-binding domain (LBD) is the E/F domain, which is 30–40% similar to the LBD of ERα. However, because ERRs lack essential Cys residues, they are unable to bind estrogen or its derivatives. A conserved helix motif known as AF-2, which is revealed in ERRs, is present in the LBD. The ability of the E/F domains of the three ERR isoforms to engage co-regulators without ligand interaction makes them constitutively active (Mohideen-Abdul, 2017). However, the search for ERRs' natural ligand(s) is still ongoing, as they could represent pharmacological tools to modulate ERR activity, e.g. to increase energy expenditure to combat obesity or other dismetabolic conditions. Because ERRs are basically regulators of mitochondrial energy metabolism, they are important for a number of physiological processes that either directly or indirectly depend on energy metabolism, oxidative phosphorylation (oxphos), glucose and lipid oxidation, mitochondrial biogenesis, tumour growth and dissemination and cell proliferation and differentiation (Casaburi, 2018). In the human body, they are expressed in all tissues and cell types (https://www.proteinatlas.org/ENSG00000173153-ESRRA/tissue viewed on 23 April 2024), although they are most abundant in tissues with have high metabolic needs or high energy consumption. A functional connection between ERRα and PGC-1α is suggested by the notably high expression of another transcriptional coactivator, peroxisome proliferator-activated receptor Gamma Coactivator 1-alpha (PGC-1α), in the same tissues (Schreiber, 2003). ERRα has the highest expression level in adults, followed by ERRγ, which has an intermediate expression level, and ERRβ, which has the lowest expression level.

2.7.1. ERRα: Master Regulator of Mitochondrial Function

The ERRα, the best known among the ERR family members, is essential for many energy and metabolism-related processes, especially in tissues with high energy requirements such the brain, kidney, skeletal muscle, heart, and adipose tissue (Cerutti, 2023). Furthermore, ERRα is also involved in the metabolism of immunological and bone cells, antioxidant defense, and cancer cell metabolism. The "power centers" of cells, the mitochondria, tightly regulate metabolic activity to satisfy the various energy requirements of cells under changing physiological circumstances. Nuclear receptor corepressor 1 (NCOR1) and PGC-1α are well-known inducers of mitochondrial oxidative metabolism that are widely expressed in tissues with high energy demands, such as the skeletal muscle, heart and brown adipose tissue (BAT). Since neither has the ability to bind DNA, they must interact with other transcription factors in order to bind and control downstream target genes. Huss et al. used skeletal muscle cells from ERRα/mice and ERRα overexpressing rat neonatal cardiomyocytes to demonstrate the functional cooperation between ERRα and PGC-1α in controlling energy metabolism in cardiomyocytes and in skeletal myotubes. They also showed that ERRα is in charge of the respiratory and mitochondrial metabolic effects that follow PGC-1α activation. ERRs have since been identified as important transcription factors that trigger the transcription of PGC-1α and NCOR1 and control mitochondrial oxidative metabolism (Huss et al., 2004). The expression of glycolytic genes, including glyceraldehyde phosphate dehydrogenase, phosphofructokinase, enolase 1, and hexokinase 2, which are vital for cytoplasmic glucose metabolism, is likewise regulated by ERRs (Kida, 2015).

2.7.2. Functional Collaboration between PGC-1α and ERRα

58 proteins have been shown to interact with ERRα, according to the BioGRID database (https://thebiogrid.org visited on 23 April 2024), which aggregates protein-protein interactions from several experimental investigations. These connections demonstrate the various biological activities and intricate regulatory mechanisms that ERRα plays in various tissues. The following paragraph highlights the functional significance of the PGC-1α protein-protein interaction, which was identified 20 years ago and has since been verified in a number of tissues and physio-pathological conditions (Oliveira, 2004). In its association with ERRα, PGC-1α functions on two different levels. Firstly, it is needed for ERRα expression, and then it combines with ERRα to form a complex that allows target genes to be transcriptionally activated. PGC-1α orchestrates the transcription of genes related to mitochondrial biogenesis and oxidative metabolism, increasing energy production (Yoon, 2001). It is known that physiological signals that convey increased metabolic needs, such as cold exposure, physical exercise, or fasting, regulate PGC-1α expression in a tissue-selective manner. The high ERRα expression seen in tissues including the heart, kidney, muscle, and brown fat that also highly express PGC-1α can be explained molecularly by the fact that PGC-1α enhances ERRα mRNA levels. The presence of PGC-1α-specific binding sites on the ERRα promoter region and ERRα-specific binding sites on the PGC-1α promoter enables direct and reciprocal control over each other's transcription. ERRα is a modest transcription activator when PGC-1α is not present. However, ERRα becomes a powerful transcriptional activator when PGC-1α is co-expressed. These results imply that ERRα is not constitutively active and that binding to PGC-1α is necessary for its activation. PGC-1α can interact with ERRα through either the L2 or L3 site, even though it usually recognizes the majority of tested receptors (e.g., GR, glucocorticoid receptor; TR, thyroid hormone receptor; RXR, retinoid X receptor; ER, estrogen receptor; RAR, retinoic acid receptor; HNF4, hepatocyte nuclear factor 4; PPAR, peroxisome proliferator-activated receptor) via the canonical LXXLL motif L2. The receptors engaged in particular PGC-1α actions can be dissected by using Leu-rich motifs differently. The potential use of L2 and L3 mutants of PGC-1α as useful tools for identifying the receptors recruiting PGC-1α at different promoters is highlighted by the fact that, for example, L2A mutations affect the GR-dependent but not ERRα-dependent actions of PGC-1 α.

2.7.3. SIRT1 and AMPK Regulate the ERRα/PGC-1α Axis in Myocytes and Adipocytes

A possible role for the metabolic sensors AMPK and NAD+-dependent deacetylase SIRT1in the regulation of PGC-1α and ERRα activity was hypothesized in 2009 (Cantó, 2009). Even though the molecular effects of the post-translational changes exerted by these enzymes on ERRα are as yet to be defined, more recent research from a number of in vivo models clearly indicates that AMPK, SIRT1, PGC-1α, and ERRα work together as a functional axis to adjust energy metabolism to nutrient availability and energy expenditure at the organismic and tissue levels.

When AMPK is chronically activated, the PGC-1α/ERRα axis becomes more active, converting white adipose tissue into thermogenic beige adipose tissue (Yan, 2016). This metabolic reprogramming of the adipose tissue at the organismic level causes mice to be more resilient to cold stress and to gain less weight when fed a high-fat diet. The SIRT1/AMPK/PGC-1α axis in adipocytes was found to be activated by an antidiabetic medication that inhibits tubular glucose uptake but also unexpectedly causes body weight loss. This leads to extensive remodeling of the adipose tissue (increased mitochondrial oxidative phosphorylation, fatty acid oxidation, and thermogenesis) (Yang, 2020), which is likely the cause of the observed effect on body weight.

Through improved mitochondrial energy metabolism, calorie restriction strengthens cardiomyocyte resistance to ischemic/reperfusion injury by activating the SIRT1/AMPK/PGC-1α axis in (cardio)myocytes (Ma, 2020). In a mouse model of diabetic cardiomyopathy, pharmacologic activation of the SIRT1/AMPK/PGC-1α/ERRα axis improves heart function through enhanced mitochondrial performance, whereas dysfunction of the axis results in cardiomyopathy due to decreased mitochondrial energy metabolism.

The transcriptional mechanism that triggers the transition of fiber type from glycolytic (quick twitch) to oxidative (slow twitch) in skeletal myocytes is also regulated by the SIRT1/AMPK/PGC-1α/ERRα axis (Rasbach, 2010).

2.8. Functions of ERRα in Human Organs

2.8.1. Skeletal Muscles

Similar to the heart, mitochondrial number and metabolism are critical for cell function in type I fibers of skeletal muscle. A decrease in ERRα/PGC-1α expression or function has been found to be a common characteristic of ageing or diseased muscles in a number of investigations. Kan et al. examined the gene expression profiles of ageing murine skeletal muscle and found that one of the main characteristics of the ageing muscle is a decrease in ERRα transcription, which is accompanied with a loss in mitochondrial mass and metabolic proficiency (Kan, 2021). More recently, it was demonstrated that double knocking out ERRα and ERRγ in mice caused significant alterations in muscle physiology, including marked exercise intolerance (Wattez, 2023), histological abnormalities resembling congenital myopathies, and a sharp decline in gene expression linked to mitochondrial oxidative metabolism (and thus energy production). The double KO was the only one to exhibit a severe phenotype, suggesting that ERRα and ERRγ in the skeletal muscle are functionally redundant. By activating the metabolic sensor AMPK, which can then activate PGC-1α, ERRγ overexpression alone can actually convert type II fibers into type I fibers, boosting mitochondrial oxidative metabolism (especially fatty acid oxidation) and muscle strength in mice. Based on these observations, it is fair to assume that ERRα/γ transcriptional activation should prevent the loss of muscle mass (sarcopenia) and strength (dynapenia) with ageing and improve muscular contractility in congenital myopathies (de Smalen, 2023). There is a biological basis for the well-established positive impact of moderate but consistent physical activity on muscle tonicity in the elderly, as exercise has been demonstrated to increase the transcription of the PGC-1α/ERRα pathway in aging mice. Several studies have tried using synthetic or natural substances to activate the ERR. A sports supplement called γ-Oryzanol, which is a mixture of ferulic acid esters of terpenoids that are comparable to ABA, has been demonstrated to increase muscle strength and exercise endurance in mice by upregulating the transcription of both ERRα/γ via PPARδ (Billon, 2023). Another study found that a synthetic pan-ERR agonist increased mice's physical endurance and caused a transcriptional reprogramming of type IIA muscle fibers, similar to what happens during aerobic training. Lastly, the production of a mutant version of ERRα that is resistant to phosphorylation-induced inactivation causes muscle fiber aerobic transformation and boosts mitochondrial biogenesis, metabolic fuel oxidation, and physical endurance in mice, according to a newly published study.

2.8.2. Brown Adipose Tissue (BAT)

Triglycerides are stored in white adipose tissue (WAT), where they are produced and hydrolyzed primarily by the pancreatic hormone’s glucagon and insulin for the metabolism of fatty acids, which provide energy for the entire body. Instead, brown adipose tissue (BAT) is used for the thermal conversion of metabolic energy by dissipating the mitochondrial proton gradient through the action of a particular protein known as the "uncoupler" of oxphos, or UCP-1. BAT is significantly less common than WAT in adult humans, especially in lean individuals; it is mostly found in the vicinity of the major arteries in the chest and belly, and sympathetic innervation and thyroid hormones regulate thermogenesis. Because brown adipocytes have a lot of mitochondria, it stands to reason that the PGC-1α/ERRα axis would be especially important for their function. ERRα and ERRγ regulate the expression of many genes during the differentiation of brown and white adipocytes (Kubo, 2009). Lacking all three ERR transcription factors (α, β, and γ) in mouse primary brown adipocytes, but not just one, results in a significant decrease in mitochondrial mass and oxidative capability. It also hinders the response to β-adrenergic stimulation. ERRβ is not necessary, as demonstrated by a later study that demonstrated that ablation of ERRα and ERRγ is adequate to replicate this phenotype. Another study has shown that ERRα plays a significant role in regulating the transcription of UCP-1, which is considered the hallmark protein of BAT, even though this work emphasizes the redundancy of action of ERRα and ERRγ in brown adipocytes. A work using mice with adipose tissue-specific deletion of folliculin (FLCN), a potent AMPK repressor, provides clear evidence of the crucial significance of the PGC-1α/ERRα axis in brown adipocyte activity (Yan, 2016). A brown phenotype is reprogrammed in adipocytes by constitutively active AMPK, which also activates the PGC-1α/ERRα axis. This results in increased mitochondrial mass and oxidative metabolism, transcription of uncoupling proteins, increased energy expenditure and thermogenesis throughout the animal, and resistance to weight gain brought on by a high-fat diet. In brown adipocytes, PGC-1α and ERRα require the histone deacetylase HDAC3 as a coactivator in order for UCP-1 transcription to occur. In order to increase WAT energy dissipation and decrease body weight, it has been suggested that pharmacologically activating the AMPK/PGC-1α/ERRα axis can produce "beige" traits in white adipocytes, which are significantly more prevalent than brown adipocytes in humans (Bartelt, 2014). Because of the positive systemic metabolic effects seen in animal models of diabetes mellitus and fat liver disease upon increased energy expenditure, pharmacological or nutraceutical methods to induce the browning of WAT in humans are being actively investigated in light of the global trend towards an increase in the prevalence of overweight/obese subjects in both developed and developing countries.

2.8.3. ERRα Function in Immune Response

In the innate immune response, macrophage activation causes the generation of ROS and the stimulation of mitochondrial electron transport enzymes, which eliminates phagocytosed pathogens. ERRα-deficient macrophages produce fewer ROS in response to INF-γ, which is linked to a decrease in ERRα−/−pathogen infection mortality (Sonoda, 2007). In order to induce mitochondrial gene expression, INF-γ must first activate the ERRα-PGC-1β complex, which is triggered directly by the JAK–STAT1 pathway. The cytoplasmic or mitochondrial enzymes that are part of the intracellular antioxidant defence allow ROS to be metabolized at the point of generation. Superoxide dismutase 2, thioredoxin 2, and peroxiredoxins 3 and 5 are mitochondrial antioxidant enzymes that are expressed less in ERRα−/− MEFs. Moreover, ERRα−/− MEFs lose the PGC-1α-dependent control of mitochondrial biogenesis and component metabolic enzymes (Rangwala, 2007).

It has also been demonstrated that ERRγ indirectly regulates macrophage activity by controlling intracellular iron. ERRγ upregulates hepatic expression of the hormone hepcidin in response to microbial infection, downstream of IL-6 signaling (Kim, 2014). Hepcidin, which regulates intestinal absorption and iron mobilization from liver reserves, is the main modulator of systemic iron homeostasis. Hepcidin interacts with the iron export protein ferroportin to promote cellular iron retention during inflammation, which raises intracellular iron in macrophages and causes hypoferremia in the host (Nemeth, 2006). In response to infection, macrophages produce more intracellular iron, which promotes the growth of intracellular bacteria like Salmonella and Legionella. In mice infected with Salmonella typhimurium, hepatic hepcidin expression can be inhibited by administering the ERRγ inverse agonist GSK5182. Additionally, ERRγ suppression improves the longevity of infected mice, lowers microbial growth, and cures hypoferremia. ERRα and ERRγ isoforms have different effects on macrophage activity, according to the findings thus far. T cell activation is largely dependent on lymphocyte metabolic reprogramming.

It has been demonstrated that ERRα controls genes related to lymphocyte activation and metabolism. Treg cells generate ATP through mitochondrial oxidation of lipids, while effector T cells (Teff) mostly use glucose. A metabolic reprogramming that promotes aerobic glycolysis to enable cell proliferation occurs in tandem with Teff cell activation. Teff cell activation causes an upregulation of the ERRα protein, and during activation, maximal stimulation of genes involved in glucose and mitochondrial metabolism requires ERRα transcriptional activity. Teff cell metabolic reprogramming is disrupted in ERRα−/−mice, which lowers activated Teff cell proliferation and inflammatory cytokine output. By altering the Teff response, ERRα activity inhibition, whether through XCT790 therapy or in ERRα−/−mice, lowers mortality in an autoimmune encephalitis model (Michalek, 2011). All of these results suggest targeting ERRα to affect the metabolism of macrophages and lymphocytes as a novel means to control immunological responses.

2.9. Aim of Study

Preliminary experiments, detailed in the Results section, indicated that silencing of ERRα compromised some of the effects of LANCL overexpression in cardiomyocytes. The aim of the study was to verify a possible functional collaboration between the LANCL proteins and ERRα.

3. MATERIALS AND METHODS

3.1. Cell Culture

The ATCC (LGC Standards s.r.l. Milan, Italy) provided the rat embryonic cardiomyocyte H9c2 cell line, which was then cultivated in high glucose Dulbecco's Modified Eagle Medium - DMEM (Mercks, Milan, Italy) supplemented with 10% fetal bovine serum (FBS), penicillin (62.5 µg/mL), and streptomycin (100 µg/mL). The cells were maintained in a humidified environment with 5% CO2 at 37 °C. The HEK293 Plat-A cells used to produce lentivirus and Hela 7e6 (GBB, RUG) both were cultured in same medium and conditions as of cardiomyocytes, whereas immune cells naive $CD14^+$ Monocytes and Peripheral Blood Lymphocytes (PBLs) were grown in high glucose Roswell Park Memorial Institute medium - RPMI (Sigma-Aldrich) 10% FBS and 1% 100X Anti-Anti (Antobiotic-Antimycotic) (Gibco).

3.2. Reactive Oxygen Species (ROS) Detection Assays

Intracellular and mitochondrial ROS levels were assessed using two fluorescent probes: 2',7'-dichlorodihydrofluorescein diacetate (H_2DCFDA) and MitoSOX™ Red (Gomes et al 2005; Robinson et al 2006). H_2DCFDA is a cell-permeable dye that is deacetylated by intracellular esterases and, upon oxidation by ROS, converted into the fluorescent compound DCF, serving as a general indicator of total cellular ROS. In contrast, MitoSOX™ Red selectively accumulates in mitochondria and specifically detects superoxide anions. For H_2DCFDA-based ROS measurement, H9c2 cells (1×10^4 per well) were seeded in 96-well plates and cultured overnight in high-glucose DMEM supplemented with 10% FBS and 1% penicillin–streptomycin. After a wash with HBSS, cells were incubated for 45 min at 37 °C with 10 µM H_2DCFDA in HBSS, with or without 100 nM ABA. Following incubation, cells were washed again, supplied with fresh HBSS (100 µL), and fluorescence was recorded using a Clariostar Plus plate reader (488/530 nm). For each condition, mean fluorescence was calculated from five sequential readings per well, with at least eight technical replicates. For mitochondrial ROS detection, MitoSOX™ Red (5 mM stock) was dissolved in DMSO and diluted in HBSS to obtain a 5 µM working solution. Cells were incubated with 500 µL of this solution for 20 min at 37 °C, washed with HBSS, and immediately imaged using a Leica TCS SP2 confocal microscope equipped with a 60× oil-immersion objective (NA 1.4; excitation 510 nm, emission 580 nm). Quantitative image analysis was performed in FIJI/ImageJ (version 2.14.0/1.54f) (Schneider, 2012) by measuring the fluorescence intensity within selected ROIs after background subtraction. Multiple fields and at least three independent experiments were analyzed.

3.3. Confocal Microscopy

To analyze the subcellular localization of LANCL2 and ERRα in H9c2 cardiomyocytes by confocal microscopy, the recombinant plasmids LANCL2-GFP (Fresia, 2016) and ERRα-RFP were employed. The pERRα-RFP construct was generated by amplifying the ERRα coding sequence by PCR, as described in section 3.2, using the following primers: 5’-AATTAGATCTATGTCCAGCCAGGTGGTGGGC-3’ (forward-BglII restriction site underlined) and 5’-AATTGTCGACTCAGTCCATCATGGCCTCGAGC-3’ (reverse-SalI restriction site underlined) for the cloning in the vector pTag-RFP-C (Evrogen, Vinci-Biochem, Florence, Italy). The PCR amplification, digestion with restriction enzymes, purification of PCR products, and cloning in the vector pTag-RFP-C were performed as described for the LANCL2-pBABEvector in paragraph 3.2. For transfection of H9c2 cardiomyocytes, 1.5×10^5 cells were seeded in 10 cm^2 plates containing complete DMEM and maintained at 37 °C in a 5% CO_2 incubator until they reached approximately 80% confluence. Cells were then transfected with the LANCL2-GFP and ERRα-RFP plasmids using the PolyJet DNA transfection reagent. Five hours after transfection, 100nM ABA was added or not to assess the effect of ABA on the colocalization of LANCL2 and ERRα within the cells. Cardiomyocytes transfected with the recombinant plasmids were expected to express green fluorescent LANCL2-GFP and red fluorescent ERRα-RFP, allowing their localization to be visualized using confocal microscopy. Live-cell imaging was performed using a Nikon AX-R confocal microscope equipped with a PLAN APO λD 60× OFN25 DIC N2 NA 1.42 oil immersion objective (Nikon Europe B.V., Stroombaan 14, 1181 VX Amstelveen, The Netherlands). Excitation/emission settings were 488 nm (500–540 nm) for LANCL2-GFP and 567 nm (580–640 nm) for ERRα-RFP. The pinhole size was set to 1 Airy Unit at 488 nm, and the fastest scan speed was employed to minimize photobleaching and reduce acquisition time. Pixel saturation in each channel was prevented by optimizing emission and detection parameters. Images were acquired at a resolution of 2048 × 2048 pixels with a pixel size of 0.07 µm. Spatial colocalization was assessed using two-dimensional correlation cytofluorograms generated with macro routines integrated as plug-ins in ImageJ Fiji software (Wayne Rasband, National Institutes of Health, Bethesda, MD, USA).

3.4. FRET - FLIM Analysis

FRET-FLIM microscopy combines two advanced optical techniques to investigate molecular interactions in living cells. Fluorescence Resonance Energy Transfer (FRET) detects whether two molecules are in very close proximity (within ~3 nm), while Fluorescence Lifetime Imaging Microscopy (FLIM) measures changes in the fluorescence lifetime of a donor molecule when energy is transferred to an acceptor. A reduction in donor lifetime, visualized as a shift toward blue in lifetime maps, indicates that the two molecules are closely associated. Together, FRET-FLIM provides a powerful approach for studying protein–protein interactions with high spatial and temporal resolution. For this purpose, HeLa cells (7×10^6) were cultured and transfected with the LANCL2-GFP and ERRα-RFP plasmids, with or without the addition of 100 nM ABA, and their localization was examined using a PicoQuant MicroTime 200 STED microscope. First, the culture plates and coverslips designated for HeLa cell culture (7×10^6 cells) were coated with Poly-L-lysine to enhance cell adhesion. After preparation, 2×10^5 HeLa cells were seeded onto each coverslip placed in a 24-well plate containing complete DMEM. When the cells reached approximately 80% confluence, they were transfected with the purified recombinant plasmids LANCL2-GFP and ERRα-RFP using the Polyplus jetPEI DNA Transfection Kit. Five hours after transfection, 100 nM ABA was added to the transfected HeLa cells, which were then incubated overnight at 37 °C in a humidified incubator with 5% CO_2. Twenty-four hours post-transfection, the cells adherent to the coverslips were fixed with 4% paraformaldehyde and mounted onto slides using a Trolox-based anti-fading mounting medium (70% glycerol + 100 mM phosphate buffer, pH 8.5 + 1 mM Trolox). The coverslips were then sealed with nail polish and left to dry thoroughly for 24 hours at 4 °C. FRET images were subsequently acquired using a PicoQuant MicroTime 200 STED fluorescence microscope, and image analysis was performed with FLIMfit 5.1.1 and FIJI/ImageJ software.

3.5. Lentiviral and Retroviral Transduction of H9c2 Cardiomyocytes

LANCL1-2 overexpressing H9c2 (OVL1+2) and LANCL1-2 silenced H9c2 (SHL1+2) and relative controls cells (PLV-Lentiviral Vector Plasmid and SCR-Scramble Control, respectively) were obtained as described before (Spinelli, 2023 Antioxidants) using for overexpression pBABE/LANCL1 and pBABE-LANCL2 vectors and for silencing pLV[shRNA]-Puro-U6 targeting rat LANCL1 and LANCL2 (plasmid IDs: VB181016-1107sen and VB181016-1124zjp, respectively) purchased from VectorBuilder (Chicago, IL, USA). For silencing of ERRα on H9c2 overexpressing or not LANCL1-2 proteins, lentiviral plasmids pLV[shRNA]-Puro-U6 encoding a control scramble shRNA (plasmid ID: VB010000-0005mme) and shRNAs targeting rat ERRα (plasmid ID: VB221005-1073jxq) were purchased from VectorBuilder (Chicago, IL, USA) and used for lentiviral transduction on H9c2 cells (Spinelli, 2023 Antioxidants). For overexpression of LANCL2 and ERRα on H9c2 cells, the following retroviral pBABE vectors were used: PLV-pBABE used as negative control (Addgene, Watertown, MA, USA), LANCL2-pBABE constructed as described before (Spinelli, 2021), and ERRα-pBABE. The full-length of hERRα was amplified from 1 ng of the vector pCMV flag ERRα (ID 10975, Addgene) by PCR using the following primers: 5'-

AATTGAATTCATGTCCAGCCAGGTGGTGGGC-3’ (forward-EcoRI restriction site underlined) and 5’-AATTGTCGACTCAGTCCATCATGGCCTCGAGC-3’ (reverse-SalI restriction site underlined) for the cloning in the pBABE vector. The PCR was performed in 25 µl containing 1x reaction buffer, 300 mM dNTP, 7.5 pmol of primers, and using 2.5 units of Pfx50 DNA Polymerase (Thermo Fisher Scientific, Milan, Italy). The PCR reaction profile was 1 cycle at 94 °C for 1 min, 35 cycles at 94 °C for 30 s, 60 °C for 30s, and 72 °C for 30 s with a final extension for 5 min at 72 °C. The PCR products were purified from agarose gel with a QIAEX II Gel Extraction Kit (Qiagen), digested with EcoRI and SalI, and cloned into pBABE using a Rapid Ligation Kit (Roche, Milan, Italy). The pBABE/ERRα vector was purified using Plasmid Mini Kit (Qiagen), sequenced by BMR Genomics (Padova, Italy), and used to transform *E. coli* BL21 (Agilent Technologies, Milan, Italy). To generate H9c2 cells stably overexpressing LANCL2 and ERRα (OVL2+ERRα), retroviral transduction was performed as described before (Spinelli et al 2023). Briefly initially, HEK293 Plat-A cells were plated in Dulbecco's modified Eagle media supplemented with 0.1% penicillin-streptomycin and 10% fetal bovine serum (Complete DMEM) at a density of 3 × 10^5 cells per 6 cm plate (Plate A). When they had reached 70% confluency, cells were transfected with 1µg of plasmid DNA using PolyJet DNA transfection Reagent (Tebu-bio, Milan, Italy). Also, in parallel, 7 × 10^5 H9c2 cardiomyocytes were plated in 10cm plate (Plate B) and incubated till it reached 80% confluency. The first infection was performed after 24 hours and 2nd infection after 48 hours post transfection of HEK293 Plat-A cells by transferring lentivirus rich medium from plate A to plate B (H9c2 cardiomyocytes) using 0.45 µm syringe filter (Fig. 5) along with addition of 5 µg/ml Protamine sulphate in plate B for each infection (Figure 5). Then, puromycin at a dosage of 4µg/ml was used to select infected cardiomyocytes following the second infection cycle. Western blot analysis was used to determine transduction efficiency 72 hours after selection.

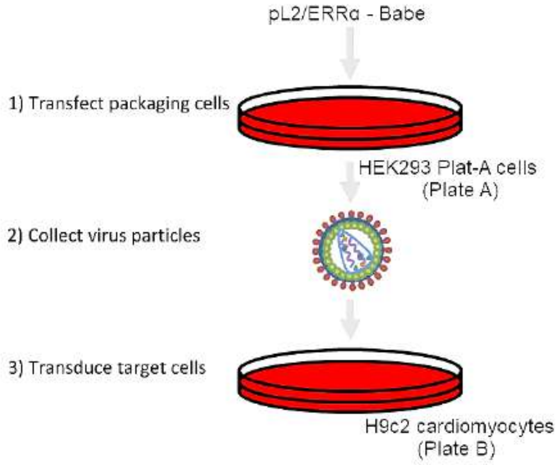

Figure 5: Steps of Transduction infection. It includes transfer of lentivirus (containing *human LANCL2* and *human ERRα* gene) rich medium from HEK293 Plat-A (Plate A) to H9C2 cardiomyocytes (Plate B).

3.6. qPCR Analysis

Total RNA was extracted from rat H9c2 cariomyocytes using RNeasy Micro Kit (Qiagen, Milan, Italy) according to the manufacturer’s instructions. The cDNA was synthesized by using High Capacity cDNA Synthesis Kit (ThermoFisher Scientific, Monza, Italy) starting from 2µg of total RNA and was used as a template for qPCR analysis: reactions were performed in a QuantStudio1 Real-Time PCR System (ThermoFisher Scientific, Monza, Italy). The rat-specific primers were designed using the tool Pick Primers on National Center for Biotechnologies Information (NCBI) database and their sequences are listed in Table 1. Each sample was assayed in triplicate in a 25µl amplification reaction, containing 4ng of cDNA, primers mixture (0.4µM each of sense and antisense primers) and 12.5µl of 2X PowerUp™ SYBR™ Green Master Mix (ThermoFisher Scientific, Monza, Italy). The amplification program included 40 cycles of two steps, each comprising heating to 95°C and to 62°C, respectively. Fluorescence products were detected at the last step of each cycle. To verify the purity of the products, a melting curve was produced after each run. Values for mouse and rat genes were normalized on Hypoxanthine-guanine Phosphoribosyltransferase-1 (Hprt1) and TATA-Box Binding Protein (Tbp) mRNA expression. Statistical analysis of the qPCR was performed using the QuantStudioTM Design & Analysis Software version 1.5.2 based on the 2-△△Ct method (Livak et al 2001). The dissociation curve for each amplification was analyzed to confirm the absence of nonspecific PCR products.

Table 1: Primers Designed Based on NCBI database

Rat genes	Accession N°	Forward Primer 5’-3’	Reverse Primer 5’-3’
Lancl1	NM_053723	TCTTGCTCCTCATCCTGCTCATC	CACTGTACTCGCCGAAGGTCTC
Lancl2	NM_001014187	GGTGCCACGGTGCTCCAG	CCTCGCTGCCAAATCACATCAC
Esrra	NM_001008511	CCCTGACAGTCCAAAGGGTT	CATCCTCCTCCTCCTTGTGC
Prkaa1	NM_019142	AGAAGCAGAAGCACGACGG	GAAGGTGCCGACGCCC-
Ppargc1a	NM_031347	GCACACATCGCAATTCTCCC	CTCTGCGGTATTCGTCCCTC
Sirt1	NM_001372090	CAGTGTCATGGTTCCTTTGC	CACCGAGGAACTACCTGAT
Slc2a4	NM_012751	CCAGCCTACCGCCACCATAG	TTCCAGCAGCAGCAGAGC
Pdha1	NM_001004072	GATGGAGCTAAAGGCGGATCA	TCCGTAGGGTTTATGCCAGC
Pfk1	NM_031715	AGTTGGTATCTTCACGGGCG	CATAGACACGCTCTCCCACG
Cpt1b	NM_013200	TGTCTACCTCCGAAGCAGGA	TGAACGGCATTGCCTAGACG
Nampt	NM_177928	TCGGTTCTGGTGGAGGTTTGCTAC	TCCCTGCTGGCGTCCTATGTAAAG
eNos	NM_021838	AGGCCTTGGTATTGGTGGTG	TAGGGGCCCGACATTTCCAT
Mt-nd1	KJ530565	CCACGCTTCCGTTACGATCA	GTATGGTGGTACTCCCGCTG
ANT1	D12770	TGGATGATTGCGCAGAGTGT	AATATCAGCCCCTTTCCGGC
Ucp1	NM_012682	CTTCCCTCAGGATTGGCCTC	GTCATCAAGCCAGCCGAGA

Sod2	NM_017051	TAAGGGTGGTGGAGAACCCA	ACCTTGGACTCCCACAGACA
Nox4	NM_053524	CTGTACAACCAAGGGCCAGA	GCTCTGCTCAAACACAATCCT
Gpx4	NM_017165	CCGTCTGAGCCGCTTATTGA	AATCATCGCGGGATGCACA
Cox2	S67722	GTGAAAACTGTACTACGCCGAG	TACTGTGTTTGGGGTGGGCT
Xor	NM_017154	TCCCTGCGTTTGGTAGCATC	CCAGGAAAAGAGGTGGCTCC
Tbp	NM_001439799	TCAAACCCAGAATTGTTCTCCT	TCTGCTCTAACTTTAGCACCTGT
Hprt1	NM_012583	TTGGTCAAGCAGTACAGCCC	TGGCCTGTATCCAACACTTCG

3.7. Western Blot

The puromycin selected infected H9c2 rat cardiomyocytes were cultured in 10 cm^2 plates, then were washed with Dulbecco's Phosphate Buffer Saline (PBS) and cells were lysed using 80µl of cell lysis buffer (20 mM Tris-HCl pH 7.4, 150 mM NaCl, 1 mM EDTA, 1% NP40 and Protease Inhibitor Cocktail). Cells were scraped from plates and sonicated briefly. Following an aliquot of each lysate was used to measure the protein content by Bradford Assay. After that lysate proteins were separated by SDS-PAGE (10% polyacrylamide gel). 50 µg total protein/well each sample was loaded in gel. Separated proteins in the gel were transferred onto nitrocellulose membrane (Bio-Rad, Milan, Italy) according to standard procedures. After one hour of incubation with TBST (20 mM Tris-HCl pH 7.4, 150 mM NaCl and 1% Tween 20) containing 5% non-fat dried milk, the membranes were saturated. The primary antibodies (Table 2) were then incubated for an additional hour at room temperature. Following incubation with the appropriate secondary antibodies (Table 2) and ECL detection (GE Healthcare, Milan, Italy), band intensity was quantified with the ChemiDoc imaging system (Bio-Rad, Milan, Italy). (Fig. 6).

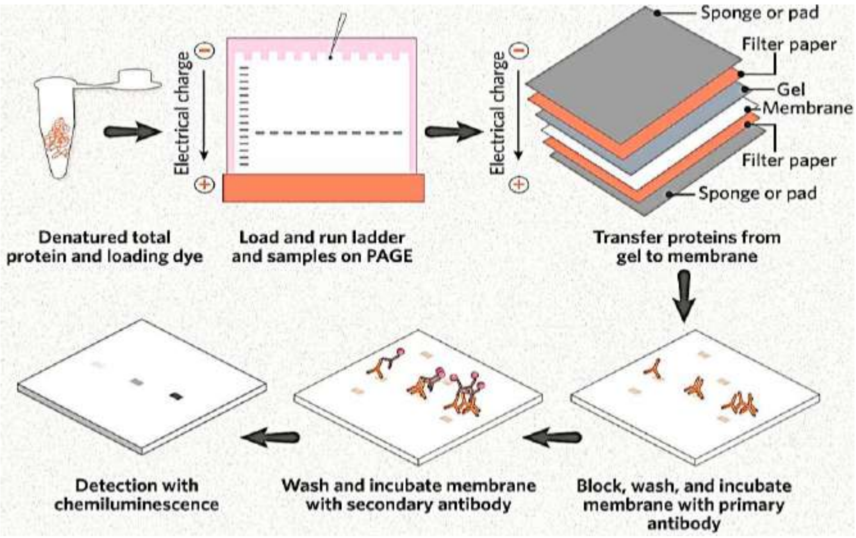

Figure 6: Scheme of Western Blotting. Cell lysate > SDS-PAGE > Blotting on membrane > Staining of membrane with antibodies.

Table 2: Primary Antibodies

Primary Antibody	**Host**	**Concentrations**	**Manufacturer**
Anti-LANCL1	Rabbit	1:250	Novus Biologicals
Anti-LANCL2	Mouse	1:1000	Reference (Vigliarolo et al 2015)
Anti-ERRα	Mouse	1:200	Santa Cruz Biotechnology Inc., California
Anti-XO	Mouse	1:100	Santa Cruz Biotechnology Inc., California
Anti-COX2	Goat	1:200	Santa Cruz Biotechnology Inc., California
Anti-SOD2	Rabbit	1:5000	Abcam
Anti-GPX4	Mouse	1:100	Santa Cruz Biotechnology Inc., California
Anti-vinculin	Rabbit	1:1000	Cell Signaling Technology, Danvers, MA
Anti-Actin	Mouse	1:1000	Santa Cruz Biotechnology Inc., California
Secondary Antibody	**Concentrations**		**Manufacturer**
Anti-Mouse	1:2000		Santa Cruz Biotechnology Inc., California
Anti-Rabbit	1:1000		Santa Cruz Biotechnology Inc., California
Anti-Goat	1:1000		Santa Cruz Biotechnology Inc., California

3.8. Expression and Purification of Recombinant Human ERRα in *E.coli*

For the expression of human recombinant hERRα protein, the ERRα coding sequence was amplified by PCR as described in paragraph 3.2, using the same PCR product and restriction enzymes, and subsequently cloned into the pGEX-6-P1 vector. Initially, *E. coli* BL21 cells containing ERRα-pGEX-6-P1 vector with the correct inserts were initially cultured in a LB broth with 200μg/ml ampicillin overnight in incubator with aeration bluffed Erlenmeyer flask until the culture reached an A_{600} of 0.4. The production of GST-ERRα fusion protein was induced by adding IPTG with final concentration 0.1 mM and incubating bacteria for 16 hours at 20°C. The bacterial cells were harvested by centrifugation and resuspended in Washing buffer then lysed by sonication. Then Triton X-100 was added to a final concentration of 1% and incubation for 30 min at 4°C. Then lysate was centrifuged at 10000xg for 15 min. The GST-ERRα- fusion protein was purified by affinity chromatography using Glutathione (GSH)-Sepharose-4B (GE Healthcare, Milan, Italy) following the manufacturer's instructions. The release of native ERRα was achieved with the PreScission Protease (GE Healthcare, Milan, Italy) by incubating the GSH-Sepharose-bound fusion protein for 16 hours at 4°C in Tris-HCl pH 7.5, 150 mM NaCl and 1 mM dithiothreitol (DTT). The native ERRα protein was concentrated through an Amicon Ultra 30 kDa (Millipore, Milan, Italy). Protein concentrations were determined by the Bradford assay (Bio-Rad, Milan, Italy) and protein purity was monitored by SDS-PAGE and by gel filtration; gel was stained with ProSieve Blue Protein Staining solution (Lonza, Milan, Italy).

3.9. Silencing and Overexpression of *LANCL2* in Immune Cells - CD14$^+$ Monocytes and Peripheral Blood Lymphocytes

LANCL2 overexpression and silencing were carried out in naïve CD14$^+$ monocytes and Peripheral Blood Lymphocytes (PBLs) to assess the impact of altered LANCL2 expression on the physiology and functional responses of these immune cells. To isolate CD14$^+$ monocytes and PBLs from blood, buffy coat was treated Ficoll Paque (ThermoFisher Scientific, Milan, Italy) to isolate Peripheral Blood Mononuclear Cells (PBMCs). The PBMCs pool is composed of PBLs (Lymphocytes T&B and Natural Killer cells) as biggest component, CD14$^+$ Monocytes, and Dendritic cells (smaller component). From PBMCs pool, CD14$^+$ Monocytes were separated from PBLS with the use of CD14$^+$ MicroBeads - Magnetic Activated Cell Sorting (MACs) (Miltenyi Biotec., Bologna, Italy). For LANCL2 overexpression in CD14$^+$ monocytes and PBLs, the pBluescript hLANCL2-SK plasmid was generated using the pBluescript-SK vector (provided by the Groningen Biomolecular Sciences and Biotechnology Institute, Netherlands – GBB). Briefly, the LANCL2 coding sequence was amplified by PCR using the following specific primers: 5’-ATAT<u>TTAATTAA</u>GCCACCATGGGCGAGACCATGTCAAAG -3’ (forward-PacI restriction site underlined) and 5’- AATT<u>CTCGAG</u>TTAATCCCTCTTCGAAGAGTCAAG -3’ (reverse-XhoI restriction site underlined) for the cloning in the plasmid pBluescript-SK. The resulting hLANCL2-SK recombinant plasmid was used to transform 5α competent E. coli, after which the transformed colonies were expanded and the plasmid was purified using the Nucleobond Xtra plasmid purification kit (Qiagen, Milan, Italy). In next step, pBluescript LANCL2-SK was used to synthesize LANCL2 mRNA with T7 promoter to overexpress the LANCL2 protein in the LANCL2 mRNA transfected immune cells. For this, initially pBluescript LANCL2-SK was linearized with Xbal through CutSmart restriction enzyme protocol followed by purification of linearized plasmid DNA purification with NucleoSpin Gel and PCR Clean-up kit (Qiagen, Milan, Italy). Later, the purified linearized pBluescript LANCL2-SK was transcribed into LANCL2 mRNA using High Yield T7 Anti-Reverse Cap Analog (ARCA) mRNA synthesis kit (Jena BioScience, Germany). Then, this mRNA was purified by using DNAse I and Lithium Chloride (LiCl) precipitation method. For overexpression of LANCL2, these cells were transfected with LANCL2 mRNA and mScarlet RNA Control. Controls used for overexpression experiments were already constructed and provided by Groningen

Biomolecular Science and Biotechnology Institute Netherlands - GBB. For LANCL2 silencing in CD14$^+$ monocytes and PBLs, a human LANCL2-specific siRNA (ID 109155, Life Technologies Italia, Milan, Italy) was employed in parallel with scramble siRNA (Stealth siRNA Control, Life Technologies Italia, Milian, Italy). Transfection was performed using Microporation with NEON Transfection system (ThermoFisher, Milan, Italy). For transfection, cells were divided into two batches to apply following parameters for microporation, voltage: 1000v (for 1st batch of cells) and 1400v (for 2nd batch of cells), width 40mS, pulse 2. Five hours after transfection, 0.1 µM ABA was addet or not and incubated overnight. After 30 hours, cells were lysed for protein expression analysis by Western Blot analysis. It is important to note that CD14$^+$ monocytes and PBLs transfected for LANCL2 silencing were originally intended for analysis by Western blotting to assess the reduction in protein expression. In contrast, cells transfected for LANCL2 overexpression were planned for evaluation by flow cytometry. However, these cells showed reduced viability and signs of distress after electroporation, making them unsuitable for flow cytometric analysis. Consequently, Western blotting was also performed on the overexpression samples instead of flow cytometry. This outcome highlights the need for further optimization of electroporation-based transfection protocols to improve post-transfection viability and ensure more reliable results in future experiments. Therefore, all cells were lysed using 1× Protease Inhibitor–supplemented Radio Immunoprecipitation Assay (RIPA) buffer and subsequently processed for Western blot analysis.

4. RESULTS

4.1. The ABA/LANCL1-2 Hormone/Receptors System Regulates NO and ROS Metabolism in Cardiomyocytes through ERRα

Results that were conducive to my studies indicated that ABA and its receptors, LANCL1 and LANCL2, control how cardiomyocytes react to hypoxia by triggering the production of NO. By increasing transcription, phosphorylation, and eNOS activity, LANCL1/2 overexpression in cardiomyocytes enhances cell viability during hypoxia/reoxygenation through the AMPK/PGC-1α axis (Spinelli, 2022).

4.1.1. The Transcriptional Activation of eNOS and the Resulting Increase in NO Production Induced by the ABA/LANCL1–2 system in Cardiomyocytes are Mediated by ERRα

In H9c2 rat cardiomyoblasts, LANCL1 and LANCL2 overexpression or silencing, with or without ABA, was investigated in relation to mitochondrial function, cell cycle, and the expression of cytoskeletal, contractile, and ion channel proteins. While silencing decreased the number of mitochondria, oxphos complex I, proton gradient, glucose and palmitate-dependent respiration, transcription of uncoupling proteins, and expression of proteins involved in cytoskeletal, contractile, and electrical functions, overexpression of LANCL1/2 markedly increased all these parameters (Spinelli, 2023 Antioxidants).

It was hypothesized that ERRα could be part of the signaling pathway downstream of the LANCL proteins, as it is known to control mitochondrial biogenesis and respiration via the AMPK/PGC-1α axis (see Introduction). Indeed, experimental results confirmed that ERRα transcription is controlled by the levels of expression of LANCL1/2 proteins: in LANCL1/2 overexpressing H9c2 rat cardiomyocytes ERRα mRNA was significantly higher compared with levels in control cells, transfected with the empty vector (Fig. 7); conversely, mRNA levels for ERRα were significantly reduced in double silenced cells, compared with controls, transfected with the scrambled sequence for ERRα. The combination of these opposite transcriptional trends results in approx. 20-times higher levels of ERRα transcription in LANCL1/2-overexpressing vs. -silenced cardiomyocytes (Fig. 7). An increased production of nitric oxide (NO) in LANCL1/2-overexpressing cardiomyocytes had been previously demonstrated to play a causal role in the enhanced resistance of these cells to hypoxia/reoxygenation, in terms of increased mitochondrial proton gradient, respiration, and vitality compared with double-silenced cells (Spinelli, 2022). Interestingly, the transcription of ERRα appears to be NO-dependent: in the presence of the NOS inhibitor L-NAME, mRNA levels for ERRα were reduced by approx. 70% in LANCL1/2-overexpressing H9c2 (Fig. 7). These results suggested a possible role of ERRα in the LANCL1/2-mediated mechanisms that protect cardiomyocytes from reactive oxygen species (ROS)-mediated damage following reoxygenation.

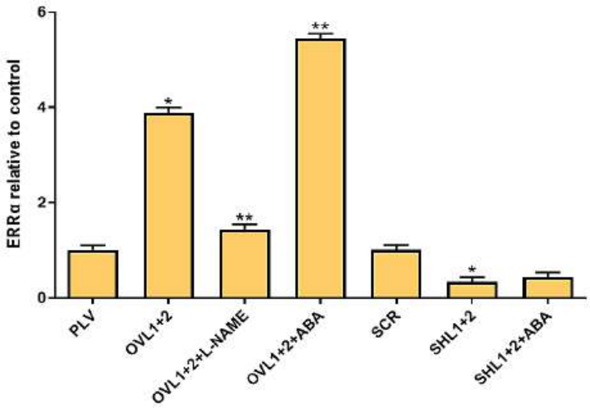

Figure 7: Regulation of NO Production by ABA-LANCL1/2 System. ERRα-dependent transcriptional responses in H9c2 cells overexpressing LANCL1/2. ERRα transcript levels in H9c2 cells overexpressing LANCL1 and LANCL2 and incubated for 4 h either without treatment or with 100nM ABA or 100µM L-NAME. ERRα expression was also measured in LANCL1-2 silenced cells, treated or not with 100nM ABA for 4 h. Data are presented relative to the corresponding control groups (PLV or SCR). *p < 0.05 versus the respective untreated controls (PLV or SCR); **p < 0.01 versus OVL1+2 cells (unpaired t-test). Values represent the mean ± SD of three independent experiments per group.

Silencing ERRα in H9c2 cardiomyocytes (SHERRα, which do not overexpress LANCL1/2) enabled us to assess whether a reciprocal transcriptional regulation exists between ERRα and the LANCL proteins. Notably, ERRα knockdown markedly decreased the endogenous transcription of LANCL1 and LANCL2 by approximately 75%, and it also abolished the ABA-induced upregulation of LANCL1/2 expression (Fig. 8). These findings indicate that ERRα and the LANCL proteins engage in a reciprocal transcriptional activation loop.

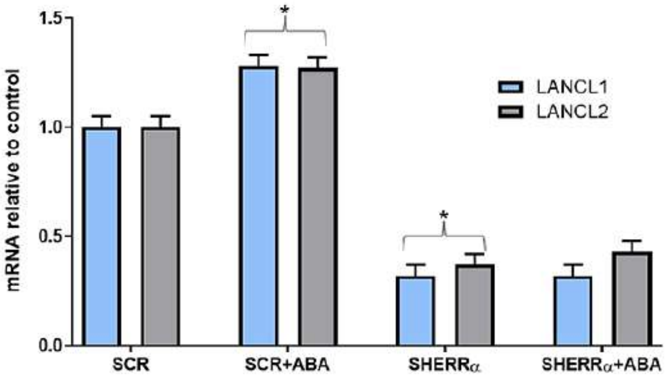

Figure 8: mRNA Expression in Transfected Cells. mRNA levels of LANCL1 and LANCL2 in untransformed H9c2 cardiomyocytes silenced for ERRα expression (SHERRα; not overexpressing LANCL1/2) and incubated for 4 h either without treatment or with 100nM ABA. p < 0.05 compared with SCR untreated cells (unpaired t-test). Data represent the mean ± SD of three experiments.

As shown in Fig. 9, the knockdown of ERRα in LANCL1/2-overexpressing cells (OVL1+2-SHERRα), in which ERRα mRNA levels are naturally fourfold higher than in PLV-infected cells due to LANCL protein overexpression (Figure 8), was evaluated by both immunoblotting (Fig. 9, left panel) and qPCR (Fig. 9, right panel). In these cells, ERRα silencing resulted in a comparable ~75% decrease in both protein abundance and mRNA levels relative to OVL1+2-SCR controls (Fig. 9).

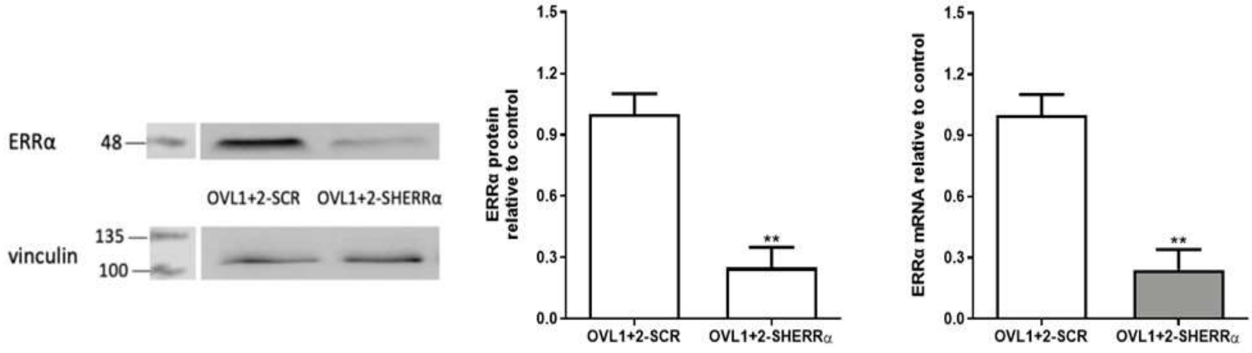

Figure 9: Comparison of Protein and mRNA Expression. Left panel: representative Western blots of ERRα protein in ERRα-silenced, LANCL1/2-overexpressing H9c2 cells (OVL1+2-SHERRα) compared with control cells (OVL1+2-SCR). Center panel: densitometric analysis of ERRα protein levels relative to OVL1+2-SCR. Right panel: ERRα mRNA levels in OVL1+2-SHERRα cells relative to OVL1+2-SCR. All values are normalized to vinculin. $p < 0.01$ compared with OVL1+2-SCR control cells (unpaired t-test). Data represent the mean ± SD of three independent experiments per group, with each measurement performed in triplicate.

We then examined how ERRα silencing affected the transcription of genes belonging to the signaling cascade downstream of the ABA/LANCL system, specifically, the AMPK/PGC-1α/Sirt1 axis. In LANCL1/2-overexpressing cells subjected to ERRα knockdown (OVL1+2-SHERRα), the mRNA levels of these genes were markedly reduced (by ~90%) compared with cells transfected with scrambled sequences (OVL1+2-SCR) (Figure 5C, upper panels). Indeed, the transcription of glucose transporter GLUT4, of glycolytic enzymes (phosphofructokinase1, PFK1, glyceraldehyde dehydrogenase, GAPDH, pyruvate kinase, PK), of subunit one of pyruvate dehydrogenase (PDHα1, required for pyruvate entry into the Krebs cycle), of protein involved in fatty acid transport (carnitine palmitoyltransferase, CPT1β) exhibited a similarly pronounced reduction (>80%) in their mRNA expression in ERRα-silenced, LANCL1/2-overexpressing cells relative to OVL1+2-SCR controls. (Fig. 10).

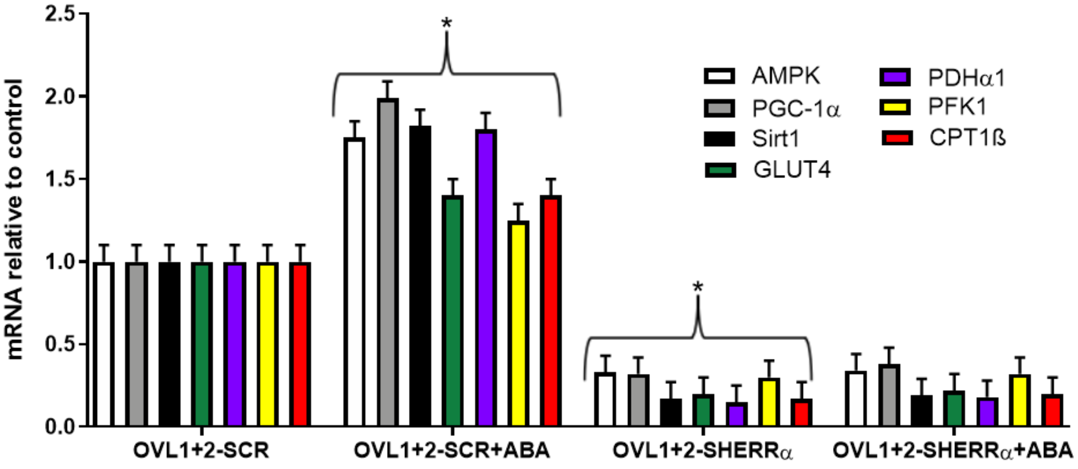

Figure 10: Effect of ERRα silencing on the transcription of metabolism-related cytosolic proteins controlled by the ABA/LANCL system. qPCR analysis of the transcription of specific genes on OVL1+2-SHERRα H9c2 and incubated in the absence or in the presence of 100 nM ABA for 4 h. Expression of AMPK, PGC-1α, Sirt1, GLUT4, PDHα1, PFK1 and CPT1ß mRNA levels.

Moreover, ERRα knockdown in LANCL1/2-overexpressing cells led to a severe suppression of transcripts involved in mitochondrial function as MT-ND, subunit 1 of complex I of the respiratory chain, the adenine nucleotide translocator ANT1, which is necessary to allow ADP/ATP exchange across the inner mitochondrial membrane, but also mediates fatty acid transport that partly dissipates the proton gradient, and the uncoupling protein UCP1. Interestingly mRNA levels of NAD-synthesizing NAMPT and of NO-producing eNOS were also significantly downregulated in ERRα-silenced, LANCL1/2-overexpressing cells relative to OVL1+2-SCR controls (Fig. 11). Thus, ERRα regulates eNOS transcription, and NO in turn enhances ERRα expression (Fig. 7).

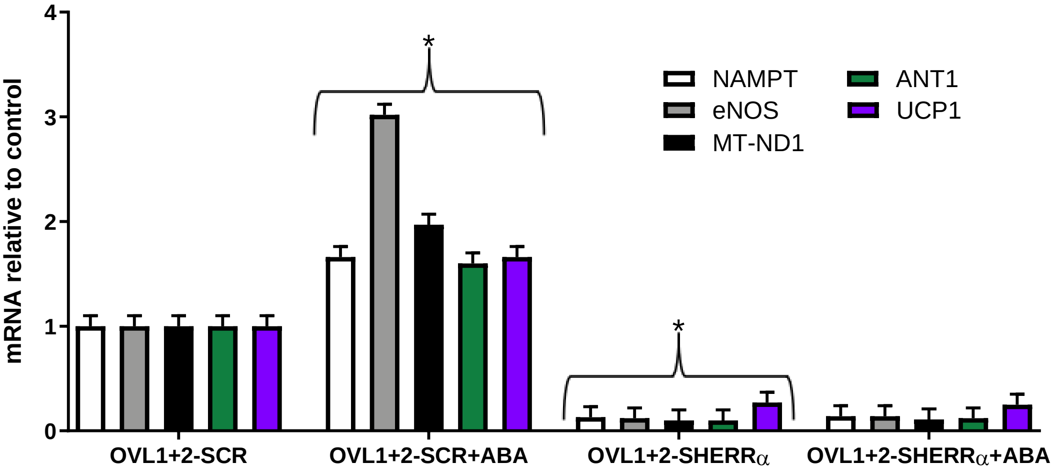

Figure 11: Effect of ERRα silencing on the transcritpion of mitochondrial energy metabolism-related genes controlled by the ABA/LANCL system. qPCR analysis of the transcription of specific genes on OVL1+2-SHERRα H9c2 and incubated in the absence or in the presence of 100 nM ABA for 4 h. Expression of NAMPT, eNOS, MT-ND1, ANT1 and UCP1 mRNA levels.

4.1.2. Role of ERRα in the LANCL1/2-Mediated Control of ROS Generation in H9c2 Cardiomyocytes

In order to investigate the role of LANCL1/2 and ERRα in ROS turnover in H9c2 cardiomyocytes, cells were retrovirally infected to induce the overexpression or silencing of LANCL1 and LANCL2, without or with the concomitant silencing of ERRα. Enzymes involved in ROS production or scavenging were studied by qRT-PCR and Western blot; mitochondrial ROS production was detected with a specific fluorescent dye. Transcription and expression of the radicals-generating enzymes cyclooxygenase-2 (COX2), xantine oxidase (XO), and NADPH oxidase-4 (NOX4) was reduced in LANCL1/2-overexpressing cells compared with controls, infected with the empty vector; conversely the same enzymes increased in double-silenced cells compared with controls, infected with the scrambled sequences of the LANCL-silencing RNAs (Spinelli, 2024 Biomedicines) (Fig. 12).

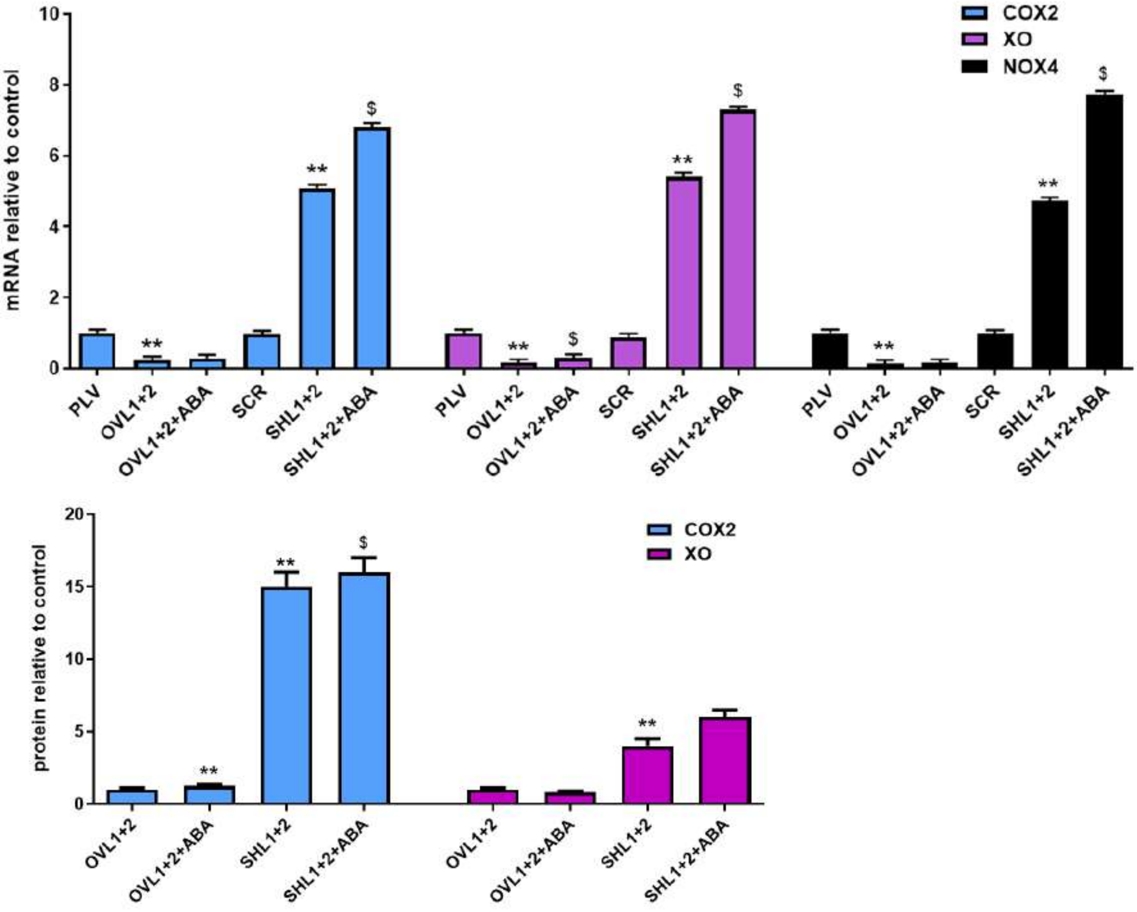

Figure 12: The ABA/LANCL system controls transcription and expression of ROS-producing enzymes in H9c2. Radicals-producing enzymes are decreased in LANCL1/2-overexpressing compared with double-silenced H9c2 cells. Upper panel: qRT-PCR analysis of COX2, XO, and NOX4 transcripts in LANCL1/2-overexpressing (OVL1+2) or LANCL1/2-silenced (SHL1+2) cells incubated with or without 100 nM ABA for 4 h. *$p < 0.001$ versus untreated controls (PLV or SCR); $\$p < 0.02$ versus ABA- OVL1+2 or SHL1+2 (unpaired t-test). Lower panel: quantification of Western

blots for COX2 and XO in LANCL1/2-overexpressing or silenced cells treated or not with 100 nM ABA, normalized to vinculin. **p < 0.001 versus untreated OVL1+2.

The ROS-scavenging enzymes superoxide dismutase (SOD) and glutathione peroxidase-4 (GPX4) instead increased in LANCL1/2-overexpressing cells relative to their controls and were conversely reduced in double-silenced cells (Fig. 13).

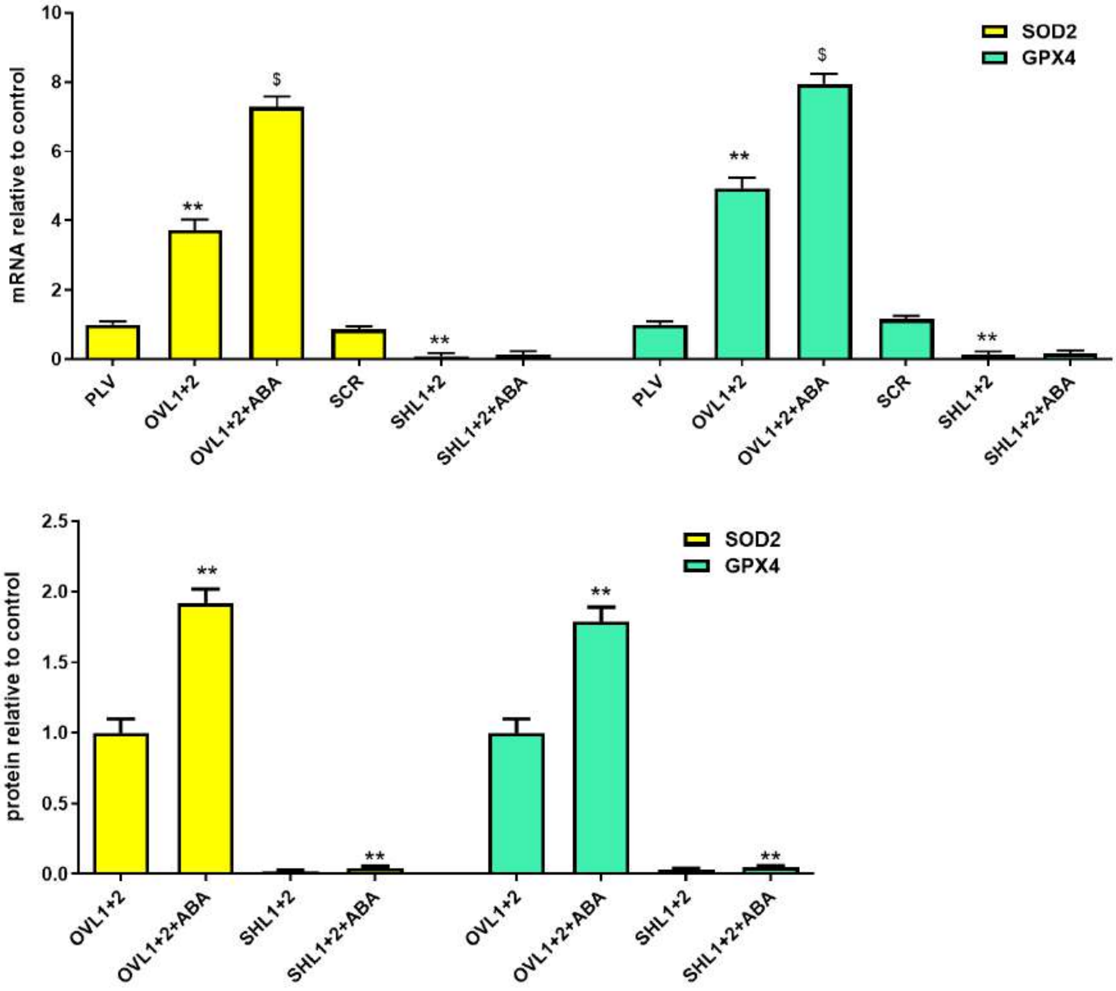

Figure 13: **The ABA/LANCL system controls transcription and expression of ROS-scavenging enzymes in H9c2.** Radical-scavenging enzymes are elevated in LANCL1/2-overexpressing compared with double-silenced H9c2 cells. Upper panel: qRT-PCR analysis of SOD2 and GPX4 expression in LANCL1/2-overexpressing (OVL1+2) or LANCL1/2-silenced (SHL1+2) cells incubated with or without 100nM ABA for 4 h. Data are shown relative to ABA-untreated PLV controls. **p < 0.001 versus untreated controls (PLV or SCR); $p < 0.02 versus ABA-untreated OVL1+2 or SHL1+2 (unpaired t-test). Lower panel: Western blot analysis for SOD2 and GPX4 in LANCL1/2-overexpressing or silenced cells, treated or not with 100 nM ABA. (mean ± SD, ≥3 experiments normalized to vinculin and expressed relative to ABA-untreated OVL1+2 cells). **p < 0.001 versus untreated OVL1+2 cells (unpaired t-test).

Silencing of ERRα in LANCL1/2-overexpressing cells significantly increased mRNA and protein levels of ROS-generating COX-2, XO and NOX4 (Fig. 14); conversely, transcription and translation of ROS-scavenging SOD and GPX4 were reduced (Fig. 15).

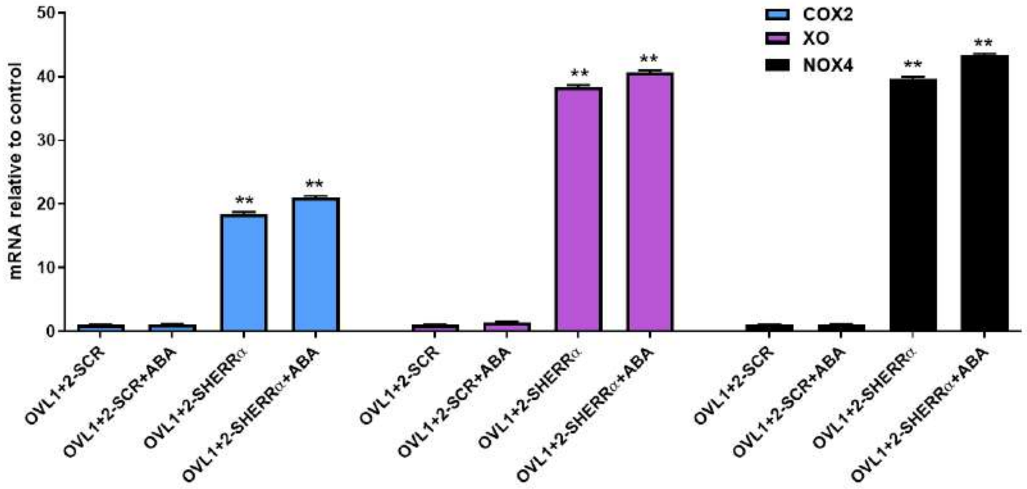

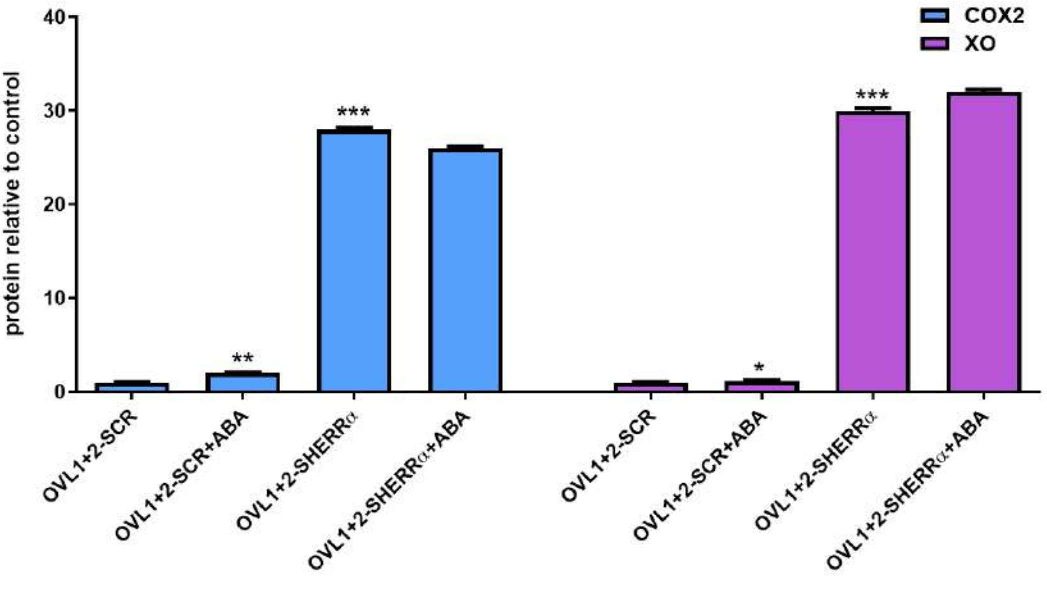

Figure 14: Role for ERRα in the ABA/LANCL-mediated effects on ROS-producing enzymes. ERRα silencing in LANCL1/2-overexpressing cells enhances radicals-generating enzymes. qRT-PCR (upper panel) and Western blot (lower panels) analyses of radicals-generating enzymes (COX2, XO, and NOX4) in OVL1+2 cells silenced for ERRα (OVL1+2-SHERRα) and incubated with or without 100 nM ABA for 4 h. Results are expressed relative to ABA-untreated OVL1+2-SCR cells. *****p < 0.001 versus ABA-untreated OVL1+2-SCR cells (unpaired t-test).

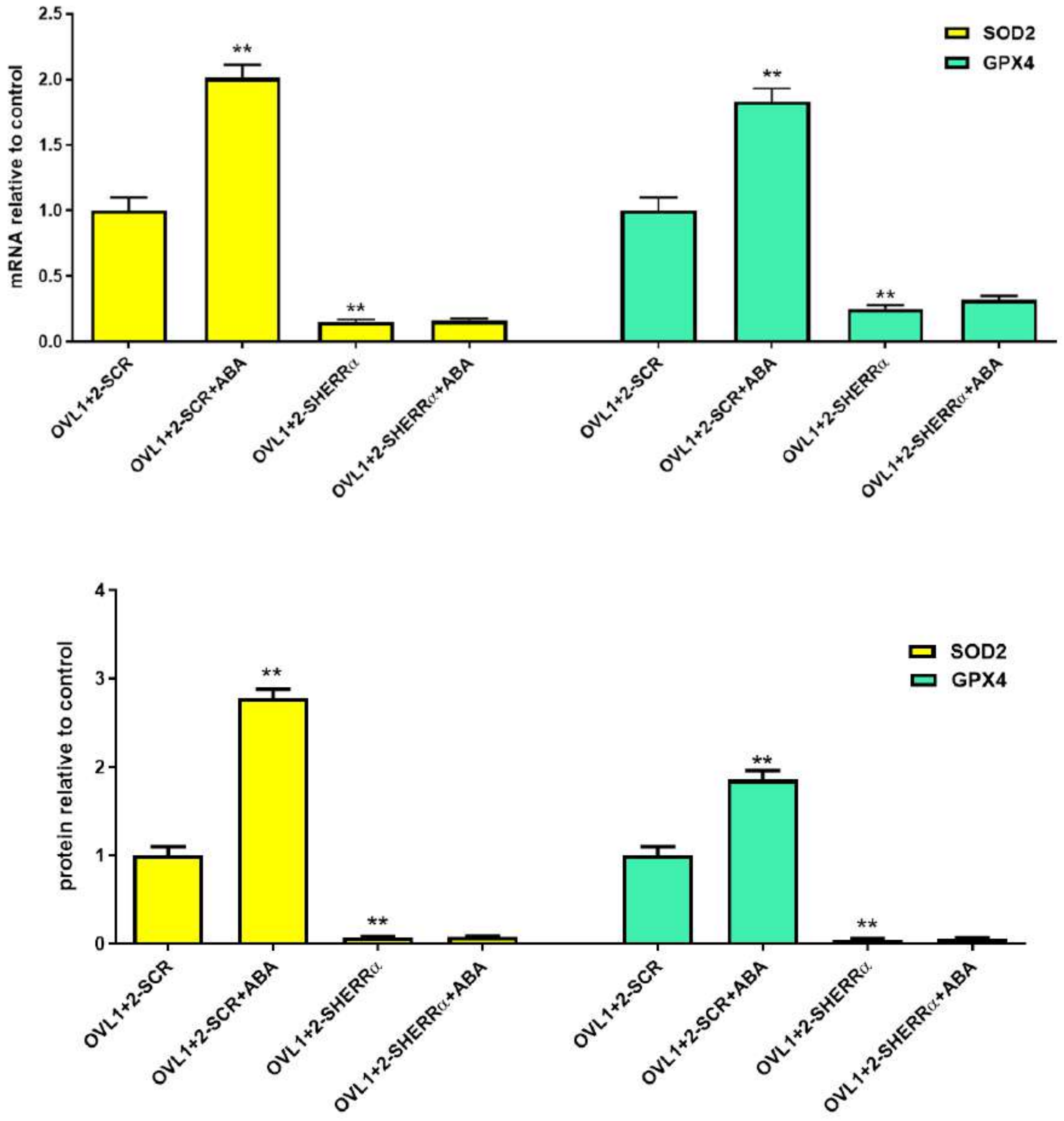

Figure 15: **Role for ERRα in the ABA/LANCL-mediated effects on ROS-scavenging enzymes.** qRT-PCR analysis (upper panel) and Western blot quantification (lower panels) of radicals-scavenging enzymes (SOD2 and GPX4) in OVL1+2 cells silenced for ERRα (OVL1+2-SHERRα) and incubated in the absence or in the presence of 100 nM ABA for 4 h. Results are expressed relative to control ABA-untreated OVL1+2-SCR cells. ** $p < 0.001$ relative to untreated OVL1+2-SCR cells by unpaired t-test.

Finally, ERRα silencing increased mitochondrial ROS production in LANCL1/2-overexpressing vs. control cells, infected with the empty vector (Fig. 16). These results indicate that ERRα is necessary to allow the protective effects mediated by the LANCL proteins against ROS-dependent oxidative stress in cardiomyocytes (Spinelli, 2024 Biomedicines).

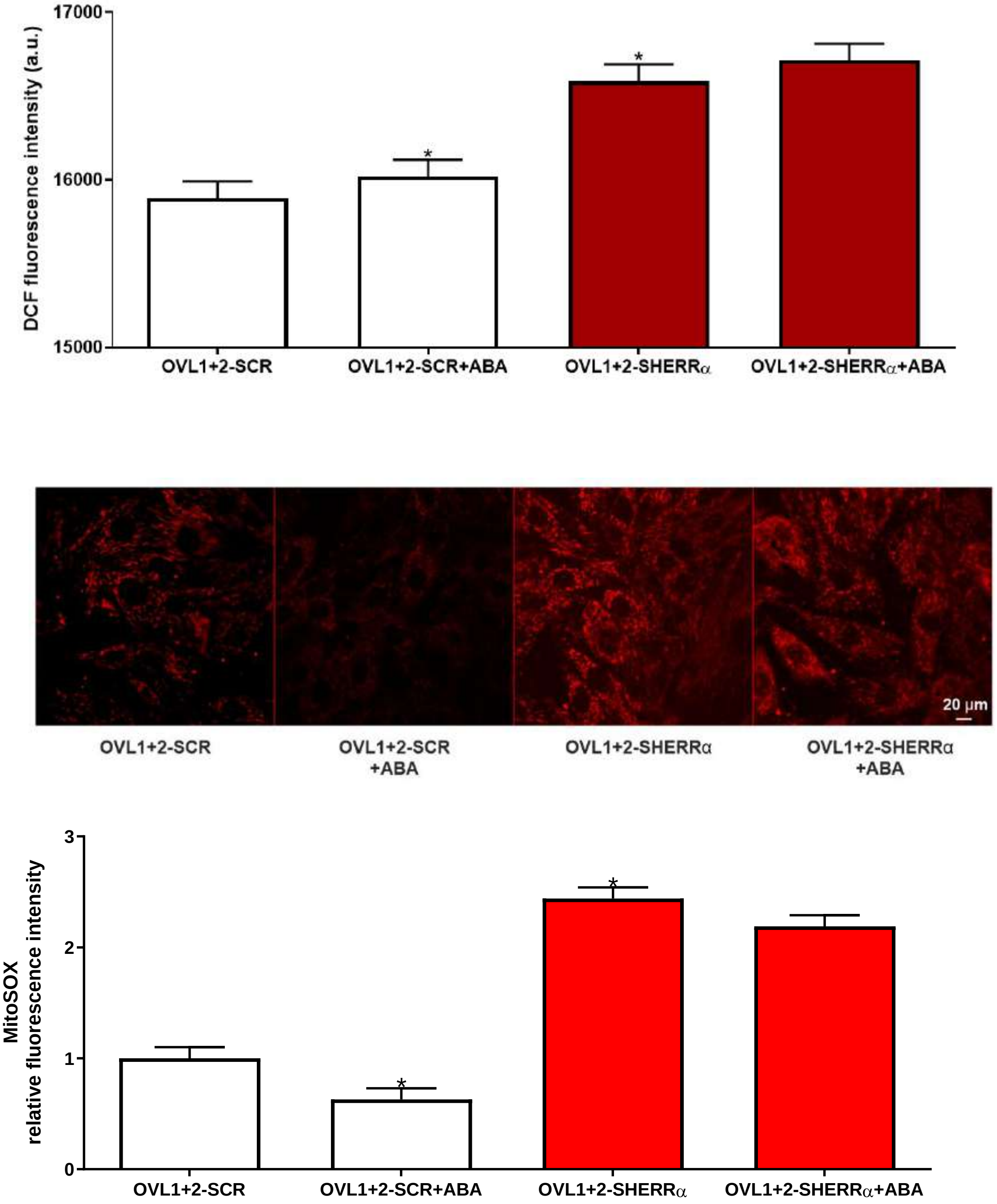

Figure 16: ERRα silencing enhances ROS production in LANCL1/2-overexpressing H9c2 cells. Upper panel: intracellular ROS levels measured by DCF fluorescence, expressed as arbitrary units relative to OVL1+2-SCR cells. Lower panel: Mitochondrial superoxide detected in MitoSOX-loaded cells by confocal microscopy in LANCL1/2-overexpressing H9c2 cells, either silenced (OVL1+2-SHERRα) or not (OVL1+2) for ERRα, after 4 h incubation with or without 100 nM ABA. Upper panel shows representative confocal images; lower panel shows quantitative data (mean ± SD of three independent experiments). $^*p < 0.01$ versus untreated OVL1+2-SCR cells (unpaired t-test).

4.2. Evidence of Co-localization of LANCL2 and ERRα in H9c2 through Confocal and FRET/FLIM Imaging

To study the subcellular localization of LANCL2 and ERRα in H9c2 cardiomyocytes by confocal microscopy, the recombinant plasmids LANCL2-GFP and ERRα-RFP were used to double transfect

H9c2 cardiomyocytes in both presence and absence of ABA (see Section 3.3) (Fig. 17). The cellular scans obtained from confocal microscopy confirm that LANCL2 localized to the plasmamembrane, to cytosolic specific site and to the nucleus, as already described (Fresia, 2016), while ERRα-RFP is localized inside the nucleus of the cells and also in the cytosol; the two proteins colocalize into the nucleus, as indicated by the presence of a yellow color inside the nucleus. The colocalization was particularly evident in the presence of 100 nM ABA (Fig. 17). Co-localization of ERRα and LANCL2 in the nucleus suggests that this interaction could be relevant in order to enable transcriptional

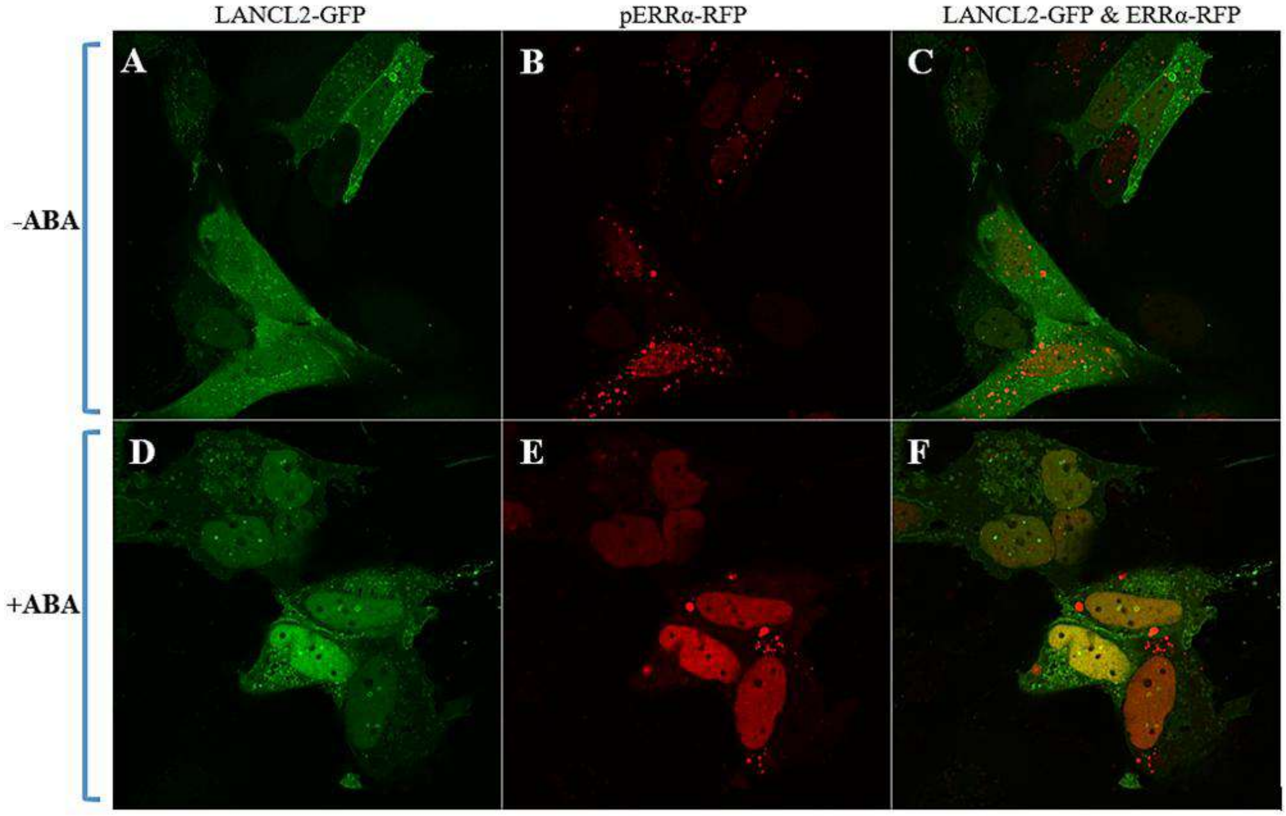

Figure 17: Confocal microscopy images of the nuclear co-localization of ERRα and LANCL2 in H9c2 Cardiomyocyte. H9c2 cardiomyocytes were double transfected with pLANCL2-GFP and pERRα-RFP in two groups, one with application of 100 nM ABA and one without ABA. A & D display the expression of only LANCL2 whereas B & E show expression of ERRα only. In C, in the absence of ABA, very poor interaction between LANCL2 and ERRα has been observed while in F, in the presence of 100nM ABA, the interaction between LANCL2 and ERRα has increased significantly represented by yellow color inside nucleus.

For the quantitative comparison of colocalization between LANCL2 and ERRα in the presence and absence of ABA, a co-localization scatterplot was generated (Fig. 18). In the absence of ABA (left panel), the plot shows a lower overlap between GFP-LANCL2 and RFP-ERRα compared with the plot obtained in the presence of ABA (right panel), which displays a pronounced clustering of signals along the 45° diagonal, reflecting strong colocalization. This shift toward the diagonal indicates that

GFP-LANCL2 and RFP-ERRα intensities increase together, demonstrating a marked ABA-dependent interaction between the two proteins.

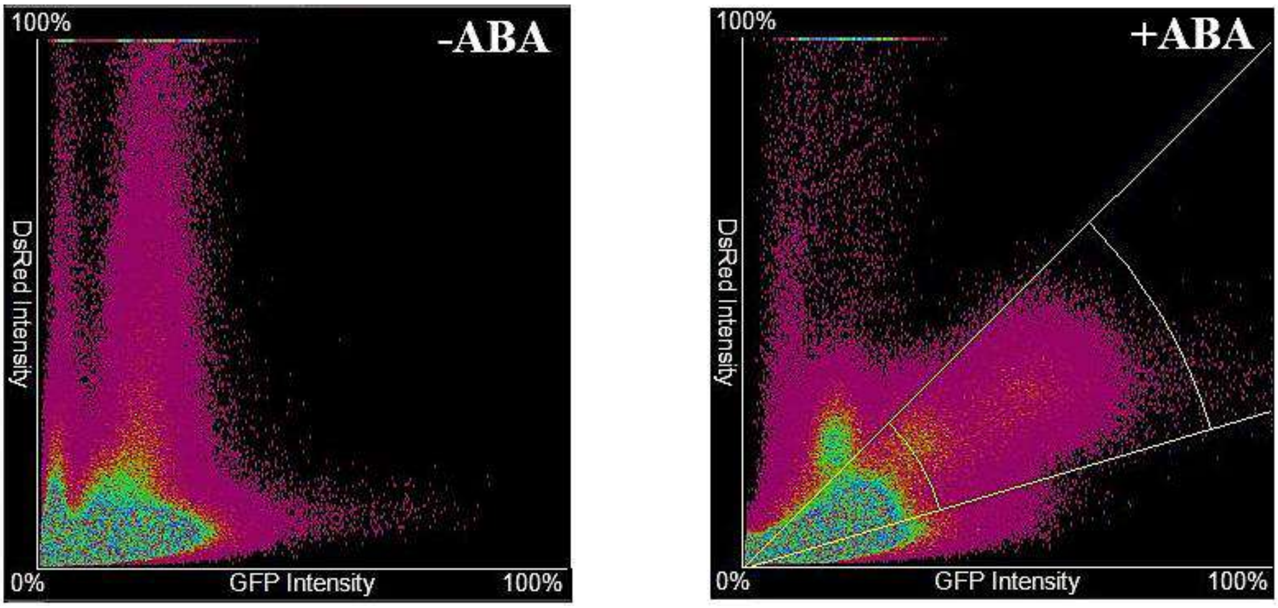

Figure 18: Co-localization Scatter Plot of ERRα and LANCL2 in H9c2. The intensity of colocalization without ABA (on the left) displays low interaction between LANCL2 and ERRα. The plot with ABA (on the right) shows increased interaction between LANCL2 and ERR demonstrating high intensity of both GFP and RFP closer to 45° angle.

After observing the co-localization of LANCL2 and ERRα in H9c2 cardiomyocytes through confocal microscopy in the H9c2 rat cardiomyocyte cell line, the FRET-FLIM analysis was done to confirm the co-localization in different cell lines. To this end, Hela cells were transfected with the plasmids for LANCL2-GFP and ERRα-RFP, cultured with 100 nM ABA and observed under a PicoQuant Microtime 200 laser microscope (see Section 3.4). FRET-FLIM analysis of Hela cells confirmed the co-localization between LANCL2 and ERRα inside the nucleus, as shown by the confocal image (Merge) at high resolution in Fig. 19. Also, the blue color in the FLIM image inside the nucleus shows a striking decrease in the life time of emitted photons, which occurs only when the electron donor (LANCL2) and the electron acceptor (ERRα) are in close proximity (3 nm or less); this fact significantly reduces the lifespan of the emitted electron, shifting the the color of the emitted light in the blue. Thus, the FRET-FLIM results confirm on transfected HeLa cells what previously observed on H9c2 cells overexpressing LANCL2 and ERRα (Fig. 17).

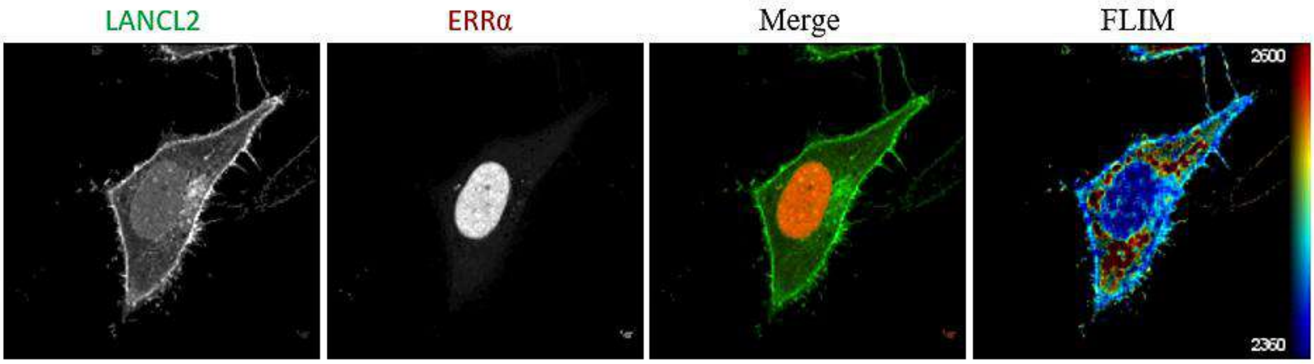

Figure 19: FRET-FLIM Scans of HeLa cells overexpressing LANCL2-GFP and ERRα-RFP. The green and red fluorescence signals emitted by the tagged proteins merge in the nucleus to give an orange fluorescence in the presence of 100 nM ABA. In the FLIM image, the blue color inside the nucleus confirms the close proximity (<3nm) of LANCL2 (electron donor) and ERRα (electron acceptor), resulting in a drop in the lifetime of emitted photons due to colocalizations.

The data analysis of drop in donor lifetime for the LANCL2-ERRα interaction in the presence and absence of ABA shows that the drop in donor lifetime in cells treated with 100 nM ABA was greater reflecting more protein-protein interaction and greater co-localization occurrence between LANCL2 and ERRα inside the cell nucleus, as compared with the cells not treated with ABA. These cells showed greater donor lifetime and hence low colocalization between LANCL2 and ERRα proteins inside the cell nucleus (Fig. 20).

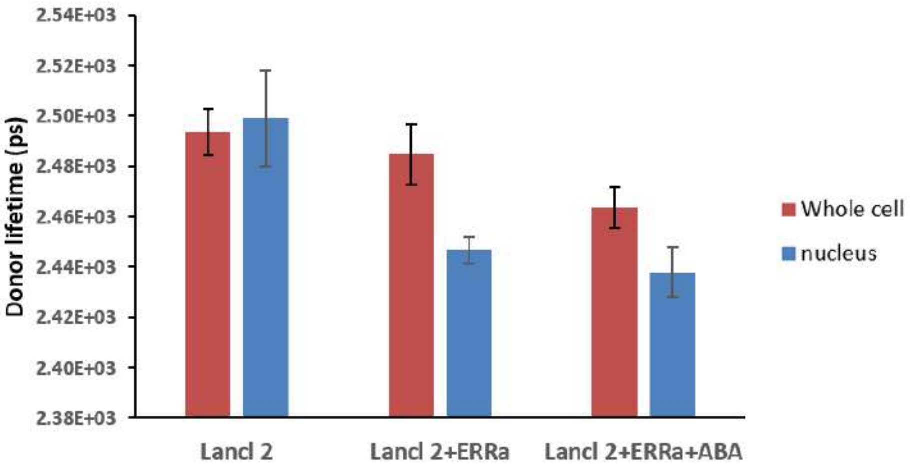

Figure 20: Comparison of donor lifetime drop in the presence and absence of ABA. Donor lifetime drop in LANCL2/ERRα-overexpressing HeLa cells treated with 100 nM ABA is greater than in cells untreated with ABA, reflecting the stronger LANCL2-ERRα interaction in the presence of 100 nM ABA.

4.3. Production of Human Recombinant ERRα and Transfection in LANCL2-Overexpressing H9c2 Cardiomyocytes

The observation that LANCL2 and ERRα co-localize in the nucleus of rat cardiomyocytes and Hela cellsboth suggested to explore whether the two proteins physically interact and also the effect of their combined overexpression on the functional activities of H9c2. Overexpression of human ERRα in LANCL2-overexpressing H9c2 was obtained using vectors ERRα-pBabe and LANCL2-pBabe by lentiviral transduction (see Section 3.5). SDS-electrophoresis analysis and Western blot of the lysates obtained from transduced cells shows a 20 and 36-folds increase of ERRα and LANCL2 expression levels respectively, as compared with control cells, transfected with the PLV (Fig. 21).

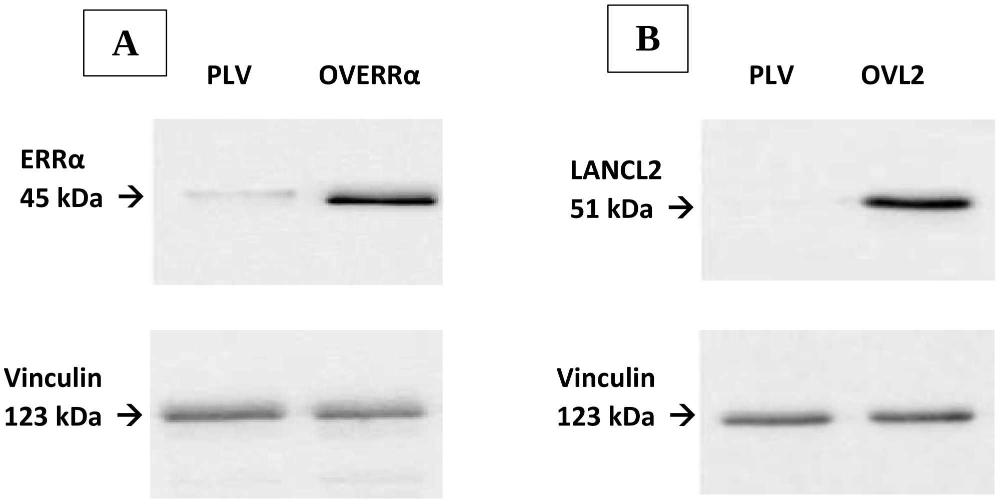

Figure 21: Western Blot of LANCL2/ERRα - overexpressing H9c2 cardiomyocytes. Human recombinant ERRα was overexpressed in LANCL2-overexpressing H9c2 cardiomyocytes through lentiviral transduction (see Section 3.5). Western blot analysis of cell lysates confirmed the significant overexpression of recombinant human ERRα, 20-fold (A) and of recombinant human LANCL2, 36-fold (B), as compared with their respective control (PLV).

The study of the functional effects of the combined overexpression of LANCL2 and of ERRα in cardiomyocytes is still underway. Preliminary results indicate that transcription of endothelial nitric oxide synthase (eNOS) and of the ROS-scavenging enzymes SOD2 and GPX4 is significantly higher in the double-transfected cells compared with H9c2 cells overexpressing only LANCL2 (not shown). Although the result of duplicate experiments was still pending when this thesis was submitted, this is in line with the observation that ERRα silencing instead produces the opposite effect, i.e. a significant reduction of the expression levels of eNOS, SOD2 and GPX4 (Fig. 11 & 15).

4.4. Production of Recombinant Human ERRα Protein in *E.coli*

Human recombinant ERRα was cloned in the PGEX-6P1 vector and *E. coli* cells were transformed with the recombinant plasmids. The recombinant protein was then purified as described in Section 3.8. A representative SDS-electrophoresis showing the result of one such purification experiment is shown in Fig. 22. The purity and the amount of the recombinant protein were adequate to perform preliminary DSC analyses, to identify the best conditions in terms of buffer and pH to ensure protein stability. These tests are still ongoing and will be followed by the addition of human recombinant LANCL2 to the ERRα sample. The type and extent of the modification to the melting curve of ERRα induced by the addition of LANCL2 (and also the other way around, the modifications induced on the LANCL2 melting curve by the addition of ERRα) will be informative regarding the possible physical interaction between the two proteins.

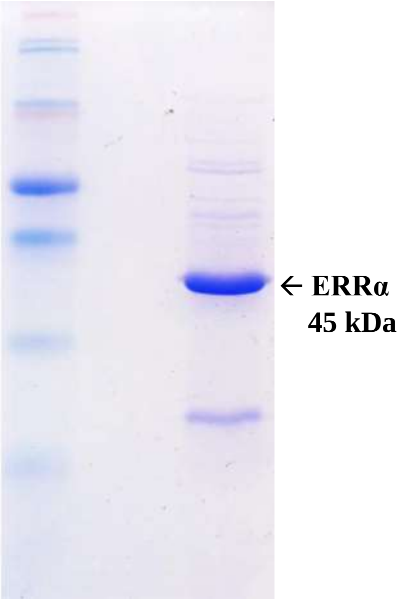

Figure 22: SDS-PAGE of Recombinant Human ERRα. SDS-PAGE of recombinant human ERRα. Human recombinant ERRα was produced in E. coli as a fusion protein with GST, purified by affinity chromatography on GSH-Sepharose, cleaved with PreScission Protease and finally concentrated (see Sec. 3.8). The figure shows a representative SDS-PAGE of a protein preparation.

4.5. LANCL2 Overexpression and Silencing in CD14$^+$ Monocytes and Peripheral Blood Lymphocytes

In order to investigate the functional role of LANCL2, and more generally of the ABA/LANCL2 system, in immune cells, the production of LANCL2-overexpressing monocytes (CD14$^+$) and lymphocytes (PBLs) was undertaken. This task was rather more complex than the transduction of continuously replicating cells, such as the H9c2 cardiomyocyte and Hela cell line, as it firstly required the purification of the cells from peripheral blood and their subsequent transfection with plasmids containing the mRNA sequence coding for human LANCL2 (1353bases) + T7promoter sequence at 5'+ untranslated region at 3' (Fig. 23).

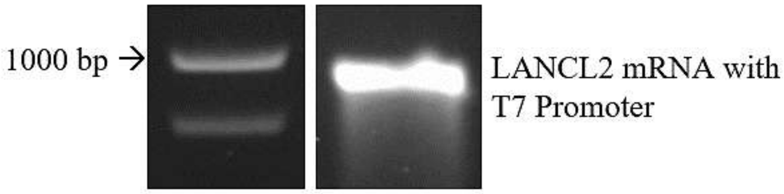

Figure 23: Purification of LANCL2 mRNA. LANCL2 mRNA was synthesized from the linearized pBluescript hLANCL2-SK DNA plasmid to transfect CD^{+14} monocytes and PBLs (by Microporation), to induce LANCL2 overexpression.

The study of the functional effects of the combined overexpression of LANCL2 and of ERRα in cardiomyocytes is still underway.

Side by side transfection of immune cells for overexpression of LANCL2 (transfected with mRNA-LANCL2) ans silencing of LANCL2 (transfected with siRNA-LANCL2) were performed. Under the applied current and pulse parameters used for microporation of CD14$^+$ monocytes and PBLs (see Section 3.9), the cells exhibited high levels of death, indicating that these conditions were detrimental. Consequently, no effective transfection or detectable signal/response was achieved for the overexpression or silencing of LANCL2 through Western blotting. The total protein concentration in the cell lysates of electroporated cells was very low. Probably low cell recovery after electroporation was the reason why neither LANCL2 nor the housekeeping gene vinculin, used for estimation of protein quantity between different cell samples, were observed at the expected MW (51 and 117 kDa, respectively, Fig. 24). This highlights the need for further optimization of microporation parameters to achieve efficient transfection while maintaining cell viability.

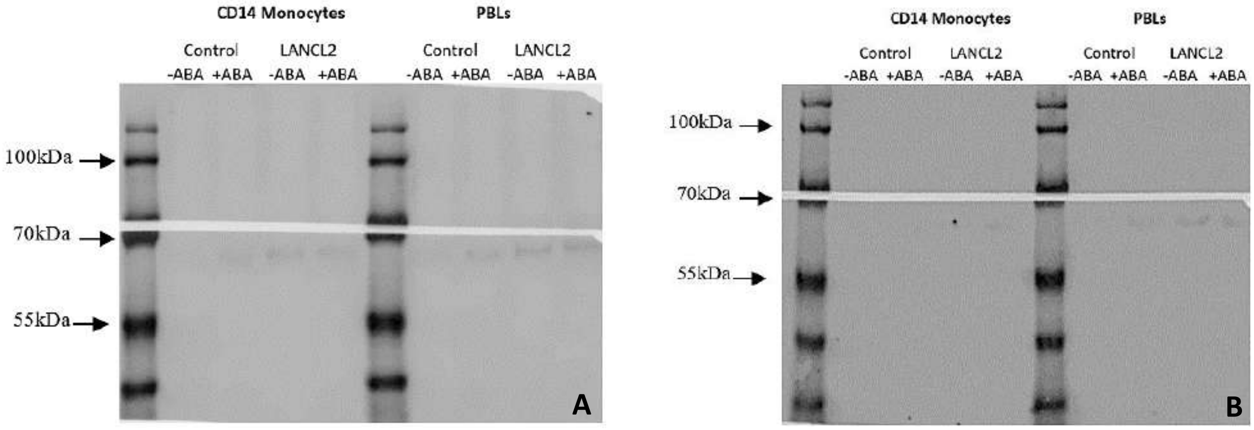

Figure 24: Western Blot of immune cells electroporated for overexpression and silencing of LANCL2. Blot A represents LANCL2 overexpression while blot B represents LANCL2 silencing. In both experiments control and LANCL2 expression altered immune cells (CD14$^+$ and PBLs) were transfected with and without 100 nM ABA treatment. The parameters applied during microporation procedure turned out to be detrimental for cell viability. Cell mortality was high, thus, total protein recovery in the cell lysates were insufficient to obtain any protein bands.

Optimization of microporation conditions for immune cells to study the functional effects of the combined overexpression of LANCL2 and of ERRα is still underway.

5. DISCUSSION

Results presented in this doctoral thesis, although still preliminary, allow to conclude that a functional collaboration between the ABA/LANCL hormone/receptors system and the transcription factor ERRα does indeed exist. This conclusion identifies the hormone ABA as an as yet unknown agonist of ERRα, through the activation of the LANCL proteins. The physiological implications of this discovery are certainly still to be fully uncovered, but what we already know about the pivotal role of ERRα in controlling energy metabolism in muscle and adipose cells suggests that the ABA/LANCL system is definitely part of the molecular mechanisms underlying these effects.

Fig. 25 summarizes the functional collaboration between the ABA/LANCL hormone/receptors system and ERRα in the control of mitochondrial activity in muscle and adipose cells

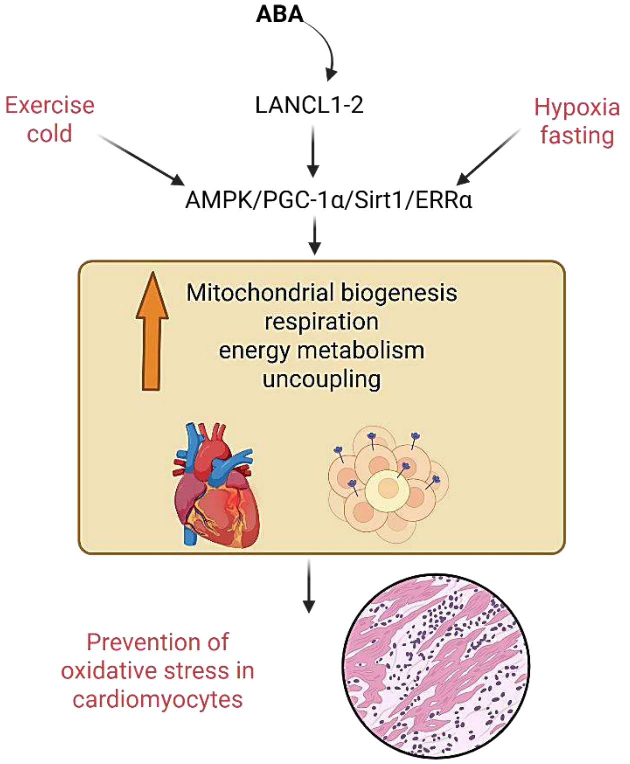

Figure 25: The ABA/LANCL hormone/receptors system controls energy metabolism via ERRalpha in myocytes and adipocytes. The ABA/LANCL1-2 hormone/receptor system activates the AMPK/PGC-1α/Sirt1 axis and the orphan-receptor/transcription factor ERRα, stimulating key mitochondrial functions like biogenesis, respiration, and oxidative phosphorylation uncoupling. This leads to increased energy availability. Various hormonal/stress signals, including ABA, hypoxia, fasting, exercise, and cold, activate this signaling pathway in physiological settings. It could be hypothesized that the ABA/LANCL signaling axis has a function in protecting against oxygen radicals, which are produced by high mitochondrial activity.

5.1. The ABA/LANCL2 Hormone/Receptor System Controls the PGC-1α/ERRα Axis in Cardiomyocytes and Adipocytes

It is interesting to note that the tissues and organs that exhibit high levels of ERRα expression include type I skeletal muscle fibers, cardiomyocytes, brown adipocytes, and neuronal cells. These tissues and organs also exhibit high levels of LANCL1 and LANCL2 transcription (https://www.proteinatlas.org/ENSG00000115365-LANCL1 accessed on 23 April 2024 and https://www.proteinatlas.org/ENSG00000132434-LANCL2 accessed on 23 April 2024). Given that skeletal myocytes overexpressing LANCL1/2 exhibit the typical functional features activated by ERRα, such as increased mitochondrial number and enhanced mitochondrial respiration via the activation of the AMPK/PGC-1α pathway, which in turn activates ERRα function and transcription with a feed-forward relay, the co-expression of the PGC-1α/ERRα axis and LANCL1/2 may have suggested their potential functional collaboration (Spinelli, 2021). Increased gene transcription and protein overexpression of the glucose transporters GLUT1 and GLUT4, the NAD-synthesizing enzyme Nampt, the RabGAP TBC1D1, and muscle-specific mitochondrial uncoupling proteins UCP-3 and sarcolipin, as well as an increased mitochondrial DNA content and respiration, are all consequences of the signaling cascade that ABA triggers via the LANCL1/2 proteins in skeletal muscle. This cascade is linked to ERRα-mediated transcriptional effects via AMPK and PGC-1α. Muscle glucose intake in vivo is raised as a result of these ABA-induced transcriptional and translational actions, which also boost muscle glucose absorption and energy metabolism. Furthermore, compared to wild-type (WT) mice, LANCL1 overexpressing and LANCL2 KO mice have higher amounts of mitochondrial DNA in their skeletal muscles as well as higher expression levels of AMPK, PGC-1α, GLUT1/4, Nampt, and UCP-3 (Magnone, 2020). These levels rise even more following the administration of ABA. Future research will probably confirm that ERRα has a part in the signaling pathway downstream of LANCL1/2 in skeletal myocytes, as seen in cardiomyocytes, even though a role in mediating these effects of the ABA/LANCL1-2 system in skeletal muscle was not investigated in this study.

5.1.1. Cardiomyocytes

The PGC-1α/ERRα transcriptional coactivator duo controls mitochondrial biogenesis and function in cardiac myocytes. ERRα is necessary for the transcriptional effects of PGC-1α on genes essential for mitochondrial energy production in cardiac and skeletal muscle. Previous research has demonstrated that the ABA/LANCL1-2 system regulates mitochondrial function in skeletal myocytes, increasing mitochondrial DNA content and respiration through a signaling pathway involving AMPK, PGC-1α, and SIRT1 (Spinelli, 2023). The overexpression of LANCL1/2 dramatically increased and the double silencing, on the other hand, decreased several important functional features of rat H9c2 cardiomyocytes. This recent study sought to understand the relationship between the ABA/LANCL1-2 system, ERRα, and mitochondrial function in cardiomyocytes. LANCL1/2 overexpression was found to have the following effects: i) increased mitochondrial respiration, with higher basal and maximal respiration rates, doubling the spare respiratory capacity, and a steeper proton gradient ($\Delta\Psi$); ii) enhanced the respiration rate fueled by fatty acids; iii) decreased mitochondrial ROS content, resulting in higher levels of ROS-scavenging enzymes and lower levels of ROS-producing enzymes; iv) increased the transcription and expression of contractile and ion channel proteins; v) improved resistance to hypoxia/reoxygenation; and vi) increased the rate of proliferation (Spinelli, 2023 Antioxidants; Spinelli, 2024 Biomedicines). Essentially, every functional characteristic of cells that overexpress LANCL1/2 is in line with the AMPK/PGC-1α/SIRT1 signaling pathway being activated. Given that ERRα silencing eliminates all transcriptional and functional effects seen in LANCL1/2-overexpressing cells, this study's identification of ERRα as a critical participant provides new information. Furthermore, it seems that ERRα and LANCL1/2 expression levels are connected via a reciprocal feed-forward transcriptional stimulation mechanism. Silencing ERRα lowers endogenous LANCL1/2 mRNA levels, whereas overexpressing LANCL1/2 enhances ERRα transcription and expression. The direct function of ERRα in cell cycle regulation is further highlighted by this study. A number of cell cycle-regulating genes, including CCNDs and E2Fs, are downregulated in double-silenced H9c2 cells and increased in LANCL1/2 overexpressing cells. ERRα plays a part in the growth-promoting function of the ABA/LANCL system, as evidenced by the detrimental effects of silencing it on the transcriptional levels of these cyclins and cardiomyocyte proliferation. These findings imply that the ABA/LANCL1-2/ERRα system functions as a novel regulator of the intricate gene network involved in cardiomyoblast energy metabolism and cell cycle progression. Since cell division necessitates large amounts of ATP, cyclins and CDKs, which are well-known for their involvement in cell cycle progression, are also essential for controlling energy metabolism. Coordinated regulation is necessary due to the tight relationship between cell division, mitochondrial activity, metabolic energy production, and nutrition availability. Further research is necessary, particularly in the context of heart pathological conditions where pharmacological stimulation of this system may have therapeutic potential, as this study shows that LANCL1/2 overexpression increases the transcription of cell cycle- and metabolism-controlling cyclins through ERRα, while their silencing has the opposite effect. Apart from converting cardiomyoblasts into "super-performing" cells, this study also reveals that LANCL1/2 overexpression protects against oxidative stress. Cells overexpressing LANCL1/2 show decreased formation of ROS in the mitochondria despite increased respiratory activity in the mitochondria, which is expected to produce ROS. The increased expression of ROS-scavenging enzymes in LANCL1/2-overexpressing cells may be partially responsible for the decreased ROS generation in these cells. ROS production significantly increases when ERRα is silenced in LANCL1/2-overexpressing cells, suggesting that ERRα is required to mediate the protective effects of LANCL1/2 on ROS creation (Scialò, 2017, Ramzan, 2020). According to these results, the ABA/LANCL1-2 system is an unknown regulator of ERRα, which in turn regulates mitochondrial energy metabolism, ROS regulation, and cell division in H9c2 cardiomyoblasts.

The study by Spinelli et al. also investigates the connection between ROS generation, respiratory chain performance, and a slight proton leak across the inner mitochondrial membrane in the setting of LANCL1/2 overexpression (Spinelli, 2024 Biomedicines). A proton leak, which is thought to improve respiratory chain performance and lower the production of ROS, is usually linked to a decrease in the proton motive force ($\Delta\Psi$) needed for ATP synthesis. LANCL1/2-overexpressing cells exhibit increased ATP-dependent respiration, but the data show a greater proton leak, which contradicts the traditional wisdom. These findings imply that a slight proton leak via ANT1 and UCP-3, whose transcription is elevated in cells that overexpress them, may actually optimize ATP synthesis. A slight proton leak facilitates electron transport by lowering the ΔG for proton pumping at respiratory complexes I and III. This prevents electrons from retrograding to oxygen, which could otherwise happen at these complexes and lead to the production of reactive oxygen species. To comprehend the molecular mechanisms behind the "fine-tuning" of oxphos shown in LANCL1/2-overexpressing cells via ERRα, more research is required.

5.1.2. Adipocytes

In brown and "beige" white adipocytes, LANCL proteins are essential for upregulating energy metabolism and mitochondrial respiration at both the transcriptional and protein levels, which supports their thermogenic and energy-dissipating properties (Spinelli, 2023 IJMS). The discovery that LANCL1/2 overexpression boosts ERRα mRNA levels in adipocytes by 20 times, while their combined silencing significantly lowers ERRα mRNA levels in both white and brown adipocytes demonstrate the direct transcriptional control of the ABA/LANCL system on ERRα in adipocytes. Furthermore, ERRα is spontaneously overexpressed in the BAT of LANCL1-overexpressing, LANCL2 KO mice, and ABA mimics ERRα expression in the BAT of WT mice. The following succinctly describes the metabolic and functional effects of the LANCL1-2/PGC-1α/ERRα axis activation in white and brown adipocytes, which is brought on by LANCL protein overexpression and further enhanced by ABA: i) increased oxidation, mitochondrial biogenesis (MT-DNA), respiration (increased expression of complex I and of basal and maximal O2 consumption), glucose transport (through GLUT4 upregulation), and ΔΨ magnitude; ii) increased expression of receptors for browning hormones (ADRβ3, THRα1/β), the enzyme deiodinase (which converts T4 into the active T3), and uncoupling proteins (UCP-1/3); iii) increased mitochondrial DNA and oxphos complex I (MT-ND1) by two and four times, respectively, in the BAT from ABA-treated mice; iv) upregulation of "browning" hormone receptors in human ABA-treated adipocytes and in the BAT from ABA-treated mice; v) LANCL1-overexpressing LANCL2 KO mice expressed more MT-ND1, thyroid hormone receptors, and ERRα than WT mice (Spinelli, 2023 IJMS). In summary, this study shows that the LANCL1/2 proteins and ERRα in brown adipocytes cooperate transcriptionally and functionally, while also suggesting possible treatment approaches to alter the metabolism and function of brown adipocytes.

5.2. ERRα: A Promising Target for Insulin Resistance and Type 2 Diabetes

ABA enhances glucose absorption in muscle and adipose tissue through LANCL1/2-mediated activation of the AMPK/PGC-1α/ERRα axis, resulting in improved glucose disposal in the face of a reduced insulin secretion by pancreatic beta cells (Magnone et al., 2020). In a regimen that included ABA pretreatment followed by diabetes induction with low-dose streptozotocin (STZ), LANCL2 KO mice had significantly lower mean glycemia than WT mice, which was attributed to LANCL1 overexpression replacing LANCL2 in ABA binding and pathway activation. Long-term ABA administration may improve muscle sensitivity to endogenous and exogenous insulin, as evidenced by the nearly 10-fold increase in insulin receptor transcription seen in WT mice treated with ABA in the same study (Magnone, 2022). Targeting ERRα should increase insulin sensitivity because ERRα is necessary for the transcriptional effects of insulin itself (Xia, 2022). In fact, a recent study reported that a non-specific ERR agonist had positive effects on an animal model of metabolic syndrome and obesity.

The identification of ABA as a putative natural regulator of glucose metabolism that functions independently of insulin makes this study significant for the treatment of diabetes. The discovery of how the ABA/LANCL1-2 system stimulates the ERRα signaling pathway to improve energy expenditure, mitochondrial biogenesis, and glucose uptake creates opportunities for novel therapeutic approaches that focus on metabolic regulation (Spinelli, 2024 IJMS). ABA provides a safer, natural alternative with fewer negative effects than traditional antidiabetic drugs, like insulin or oral hypoglycemics, which can have negative effects like hypoglycemia, weight gain, gastrointestinal distress, or cardiovascular risks. Therefore, gaining knowledge of this pathway may help create diabetes management therapies that are more efficient and well-tolerated.

5.3. Future Perspectives

New molecular tools to activate these essential master regulators of cell energy metabolism and, generally, improve cell "fitness" to its specific functional role have been made possible by the recent recognition of the role of the ABA/LANCLs hormone/receptor system in regulating the ERRα/PGC-1α transcriptional complex and fostering its genome-wide effects. It is anticipated that activation of the LANCL/PGC-1α/ERRα axis will enhance tissue and cell functions in a number of organs, with positive whole-body effects. A visual overview of this therapeutic tool is displayed in Fig. 26.

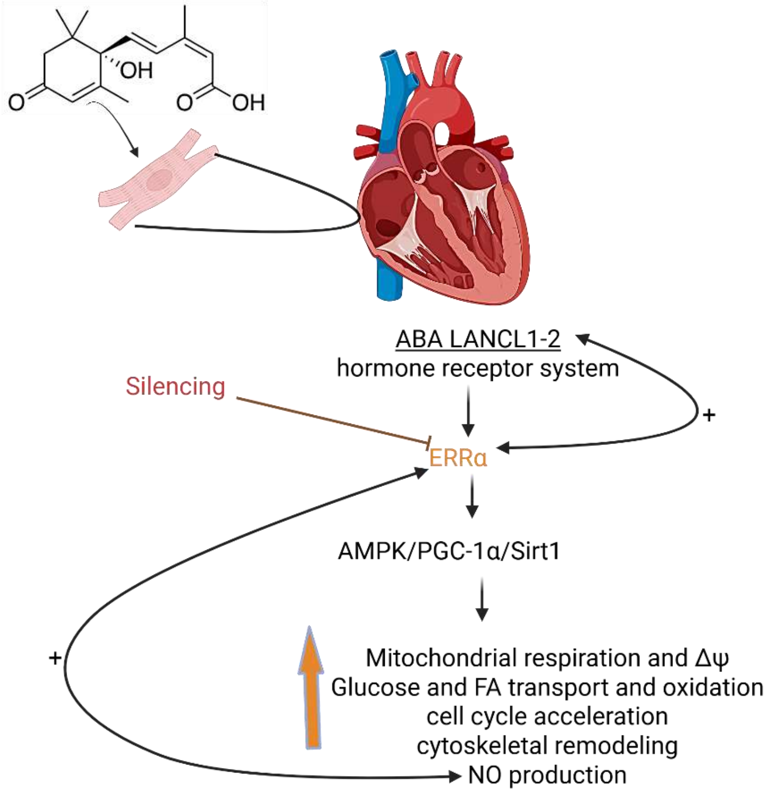

Figure 26: The LANCL/ERRα/PGC-1α axis plays a crucial role in regulating mitochondrial activity. Several processes work together to keep the LANCL1-2/AMPK/SIRT1/ERRα/PGC-1α axis active once "started". AMPK boosts Nampt activity and NAD synthesis, boosting SIRT1 activity. AMPK and SIRT1 post-translationally alter and activate PGC-1α. LANCL1/2 expression levels upregulate the expression of AMPK, ERRα, PGC-1α, and ERRα, which control LANCL1/2 expression. This signaling axis boosts mitochondrial biogenesis and oxphos activity while also improving the cell's ability to cope with increasing oxidative stress, resulting in improved respiration capacity. Environmental stressors, including as changes in food, oxygen, temperature, or cell energy status, as well as the stress hormone ABA, activate this highly conserved signaling pathway. This axis, in turn, regulates transcription of hundreds of genes involved in critical cell activities in tissues and organs with high energy needs, resulting in increased mitochondrial energy production and

antioxidant defense. These responses have an impact on the overall energy balance of the organism; hence, agonists of this signaling pathway could be employed to treat not only organ-specific disorders but also systemic conditions characterized by multi-organ failures, such as diabetes and ageing.

Several issues remain to be experimentally addressed, as always occurs when new discoveries open a new perspective on complex physiological mechanisms. The nuclear colocalization of ERRα and LANCL2 after LANCL2 translocation to the nucleus is a first information that requires further studies to conclude whether the two proteins physically interact, e.g. by forming a transcription complex, or whether their functional collaboration occurs via different mechanisms, e.g. by activation of the transcription of other proteins. It is noteworthy that ERRα, LANCL2 and PGC-1α are all transcriptionally linked; overexpression of LANCL2 increases transcription of ERRα and transcription and phosphorylation of PGC-1α, and LANCL2 silencing has opposite effects. Investigating a possible physical interaction between these proteins will require physical-chemical studies with the recombinant proteins, which are indeed underway.

Another open question regards the possible direct binding of ABA to ERRα, which could be part of the functional collaboration between ERRα and the LANCL proteins. To address this issue, in silico docking studies of ABA and ERRα and calorimetric experiments with the recombinant protein can be undertaken.

5.4. Conclusion

Through the LANCL1/2–ERRα signaling axis, abscisic acid (ABA) controls energy balance and glucose metabolism. In cardiomyocytes and skeletal muscle cells, overexpression of LANCL1 and LANCL2 increased mitochondrial biogenesis, oxidative phosphorylation, and glucose uptake, whereas silencing had the opposite effect. According to this study, ERRα is a crucial downstream effector of the ABA/LANCL1-2 pathway, mediating its transcriptional effects on genes related to cell cycle regulation, oxidative stress reduction, and energy metabolism. These results point to a hitherto unrecognized role for the ABA/LANCL1-2/ERRα axis in the activation of myocyte energy metabolism and protection from oxidative radicals and suggest that agonists of this axis may provide new treatments for pathological conditions were an increase in muscle energy metabolism could be expected to produce favorable effects, such as the metabolic syndrome, diabetes and obesity.

REFERENCES:

Addicott FT, Lyon JL, Ohkuma K, Thiessen WE, Carns HR, Smith OE, Cornforth JW, Milborrow BW, Ryback G, Wareing PF. Abscisic acid: a new name for abscisin II (dormin). *Science*. **1968**, 159, 1493.

Agelopoulos K, Greve B, Schmidt H, Pospisil H, Kurtz S, Bartkowiak K, Andreas A, Wieczorek M, Korsching E, Buerger H, Brandt B. Selective regain of egfr gene copies in CD44+/CD24-/low breast cancer cellular model MDA-MB-468. *BMC Cancer*. **2010**, 10, 78.

Ameri P, Bruzzone S, Mannino E, Sociali G, Andraghetti G, Salis A, Ponta ML, Briatore L, Adami GF, Ferraiolo A, Venturini PL, Maggi D, Cordera R, Murialdo G, Zocchi E. Impaired increase of plasma abscisic acid in response to oral glucose load in type 2 diabetes and in gestational diabetes. *PLoS One*. **2015**, 10, e0115992.

Bartelt A, Heeren J. Adipose tissue browning and metabolic health. *Nat Rev Endocrinol*. **2014**, 10, 24-36.

Bassaganya-Riera J, Skoneczka J, Kingston DGJ, Krishnan A, Misyak SA, Guri AJ, Hontecillas R. Mechanisms of action and medicinal applications of abscisic acid. *Current Medicinal Chemistry*. **2010**, 17, 467-478.

Billon C, Sitaula S, Banerjee S, Welch R, Elgendy B, Hegazy L, Oh TG, Kazantzis M, Chatterjee A, Chrivia J, Hayes ME, Xu W, Hamilton A, Huss JM, Zhang L, Walker JK, Downes M, Evans RM, Burris TP. Synthetic ERRα/β/γ agonist induces an ERRα-dependent acute aerobic exercise response and enhances exercise capacity. *ACS Chem Biol*. **2023**, 18, 756-771.

Bodrato N, Franco L, Fresia C, Guida L, Usai C, Salis A, Zocchi E. Abscisic acid activates the murine microglial cell line N9 through the second messenger cyclic ADP-ribose. *J Biol Chem*. **2009**, 284, 14777-14787.

Bruzzone S, Ameri P, Briatore L, Mannino E, Basile G, Andraghetti G, Grozio A, Magnone M, Guida L, Scarfì S, Salis A, Damonte G, Sturla L, Nencioni A, Fenoglio D, Fiory F, Miele C, Beguinot F, Ruvolo V, Bormioli M, Colombo G, Maggi D, Murialdo G, Cordera R, De Flora A, Zocchi E. The plant hormone abscisic acid increases in human plasma after hyperglycemia and stimulates glucose consumption by adipocytes and myoblasts. *FASEB J*. **2012**, 26, 1251-1260.

Bruzzone S, Moreschi I, Usai C, Guida L, Damonte G, Salis A, Scarfì S, Millo E, De Flora A, Zocchi E. Abscisic acid is an endogenous cytokine in human granulocytes with cyclic ADP-ribose as second messenger. *Proc Natl Acad Sci U S A*. **2007**, 104, 5759-5764.

Bruzzone S, Bodrato N, Usai C, Guida L, Moreschi I, Nano R, Zocchi E. Abscisic acid is an endogenous stimulator of insulin release from human pancreatic islets with cyclic ADP ribose as second messenger. *J Biol Chem*. **2008**, 283, 32188-32197.

Bruzzone S, Battaglia F, Mannino E, Parodi A, Fruscione F, Basile G, Fenoglio D. Abscisic acid ameliorates the systemic sclerosis fibroblast phenotype in vitro. *Biochem Biophys Res Commun*. **2012**, 422, 70-74.

Bruzzone S, Magnone M, Mannino E, Sociali G, Sturla L, Fresia C, Zocchi E. Abscisic acid stimulates glucagon-like peptide-1 secretion from L-cells and its oral administration increases plasma glucagon-like peptide-1 levels in rats. *PLoS One*. **2015**, 10, e0140588.

Cantó C, Auwerx J. PGC-1alpha, SIRT1 and AMPK, an energy sensing network that controls energy expenditure. *Curr Opin Lipidol*. **2009**, 20, 98-105.

Casaburi I, Chimento A, De Luca A, Nocito M, Sculco S, Avena P, Trotta F, Rago V, Sirianni R, Pezzi V. Cholesterol as an endogenous ERRα agonist: a new perspective to cancer treatment. *Front Endocrinol*. **2018**, 9, 525.

Cerutti C, Shi JR, Vanacker JM. Multifaceted transcriptional network of estrogen-related receptor alpha in health and disease. *Int J Mol Sci*. **2023**, 24, 4265.

Cichero E, Fresia C, Guida L, Booz V, Millo E, Scotti C, Iamele L, de Jonge H, Galante D, De Flora A, Sturla L, Vigliarolo T, Zocchi E, Fossa P. Identification of a high affinity binding site for abscisic acid on human lanthionine synthetase component C-like protein 2. *Int J Biochem Cell Biol*. **2018**, 97, 52-61.

Clark TN, Ellsworth K, Li H, Johnson JA, Gray CA. Isolation of the plant hormone (+)-abscisic acid as an antimycobacterial constituent of the medicinal plant endophyte Nigrospora sp. *Natural Product Communications*. **2013**, 8, 1934578X1300801203.

Dandona P, Aljada A, Bandyopadhyay A. Inflammation: the link between insulin resistance, obesity and diabetes. *Trends Immunol*. **2004**, 25, 4-7.
de Smalen LM, Börsch A, Leuchtmann AB, Gill JF, Ritz D, Zavolan M, Handschin C. Impaired age-associated mitochondrial translation is mitigated by exercise and PGC-1α. *Proc Natl Acad Sci U S A*. **2023**, 120, e2302360120.

Espinosa-Fernández V, Mañas-Ojeda A, Pacheco-Herrero M, Castro-Salazar E, Ros-Bernal F, Sánchez-Pérez AM. Early intervention with ABA prevents neuroinflammation and memory impairment in a triple transgenic mice model of Alzheimer's disease. *Behav Brain Res*. **2019**, 374, 112106.

Fresia C, Vigliarolo T, Guida L, Booz V, Bruzzone S, Sturla L, Di Bona M, Pesce M, Usai C, De Flora A, Zocchi E. G-protein coupling and nuclear translocation of the human abscisic acid receptor LANCL2. *Sci Rep*. **2016**, 6, 26658.

Giguère V. To ERR in the estrogen pathway. *Trends Endocrinol Metab*. **2002**, 13, 220-225.

Gharib A, Marquez C, Meseguer-Beltran M, Sanchez-Sarasua S, Sanchez-Perez AM. Abscisic acid, an evolutionary conserved hormone: biosynthesis, therapeutic and diagnostic applications in mammals. *Biochem Pharmacol*. **2024**, 229, 116521.

Glennon EK, Adams LG, Hicks DR, Dehesh K, Luckhart S. Supplementation with abscisic acid reduces malaria disease severity and parasite transmission. *Am J Trop Med Hyg*. **2016**, 94, 1266.

Gomes A, Fernandes E, Lima JL. Fluorescence probes used for detection of reactive oxygen species. *J Biochem Biophys Methods*. **2005**, 65, 45–80.

He C, Zeng M, Dutta D, Koh TH, Chen J, van der Donk WA. LanCL proteins are not involved in lanthionine synthesis in mammals. *Sci Rep*. **2017**, 7, 40980.

Huss JM, Torra IP, Staels B, Giguère V, Kelly DP. Estrogen-related receptor alpha directs peroxisome proliferator-activated receptor alpha signaling in the transcriptional control of energy metabolism in cardiac and skeletal muscle. *Mol Cell Biol*. **2004**, 24, 9079-9091.

Huss JM, Garbacz WG, Xie W. Constitutive activities of estrogen-related receptors: transcriptional regulation of metabolism by the ERR pathways in health and disease. *Biochim Biophys Acta*. **2015**, 1852, 1912-1927.

Hunter K, Rainbow D, Plagnol V, Todd JA, Peterson LB, Wicker LS. Interactions between Idd5.1/Ctla4 and other type 1 diabetes genes. *J Immunol*. **2007**, 179, 8341-8349.

Kan J, Hu Y, Ge Y, Zhang W, Lu S, Zhao C, Liu Y. Declined expressions of vast mitochondria-related genes represented by CYCS and transcription factor ESRRA in skeletal muscle aging. *Bioengineered*. **2021**, 12(1), 3485–3502.

Kida YS, Kawamura T, Wei Z, Sogo T, Jacinto S, Shigeno A, Evans RM. ERRs mediate a metabolic switch required for somatic cell reprogramming to pluripotency. *Cell Stem Cell*. **2015**, 16(5), 547–555.

Kubo M, Ijichi N, Ikeda K, Horie-Inoue K, Takeda S, Inoue S. Modulation of adipogenesis-related gene expression by estrogen-related receptor gamma during adipocytic differentiation. *Biochim Biophys Acta*. **2009**, 1789, 71-77.

Jiang SX, Benson CL, Zaharia LI, Abrams SR, Hou ST. Abscisic acid does not evoke calcium influx in murine primary microglia and immortalised murine microglial BV-2 and N9 cells. *Biochem Biophys Res Commun*. **2010**, 401, 435-439.

Jung Y, Cackowski FC, Yumoto K, Decker AM, Wang Y, Hotchkin M, Taichman RS. Abscisic acid regulates dormancy of prostate cancer disseminated tumor cells in the bone marrow. *Neoplasia*. **2021**, 23, 102-111.

Kan J, Hu Y, Ge Y, Zhang W, Lu S, Zhao C, Zhang R, Liu Y. Declined expressions of vast mitochondria-related genes represented by CYCS and transcription factor ESRRA in skeletal muscle aging. *Bioengineered*. **2021**, 12, 3485-3502.

Kida YS, Kawamura T, Wei Z, Sogo T, Jacinto S, Shigeno A, Kushige H, Yoshihara E, Liddle C, Ecker JR, Yu RT, Atkins AR, Downes M, Evans RM. ERRs mediate a metabolic switch required for somatic cell reprogramming to pluripotency. *Cell Stem Cell*. **2015**, 16, 547-555.

Kim DK, Jeong JH, Lee JM, Kim KS, Park SH, Kim YD, Koh M, Shin M, Jung YS, Kim HS, Lee TH, Oh BC, Kim JI, Park HT, Jeong WI, Lee CH, Park SB, Min JJ, Jung SI, Choi SY, Choy HE, Choi HS. Inverse agonist of estrogen-related receptor γ controls Salmonella typhimurium infection by modulating host iron homeostasis. *Nat Med*. **2014**, 20, 419-424.

Kinney JW, Bemiller SM, Murtishaw AS, Leisgang AM, Salazar AM, Lamb BT. Inflammation as a central mechanism in Alzheimer’s disease. *Alzheimers Dement (Transl Res Clin Interv)*. **2018**, 4, 575-590.

Le Page-Degivry MT, Bidard JN, Rouvier E, Bulard C, Lazdunski M. Presence of abscisic acid, a phytohormone, in the mammalian brain. *Proc Natl Acad Sci U S A*. **1986**, 83, 1155-1158.

Li HH, Hao RL, Wu SS, Guo PC, Chen CJ, Pan LP, Ni H. Occurrence, function and potential medicinal applications of the phytohormone abscisic acid in animals and humans. *Biochem Pharmacol*. **2011**, 82, 701-712.

Livak KJ, Schmittgen TD. Analysis of relative gene expression data using real time quantitative PCR and the 2 ΔΔCt method. *Methods*. **2001**, 25, 402–408.

Ma L, Wang R, Wang H, Zhang Y, Zhao Z. Long-term caloric restriction activates the myocardial SIRT1/AMPK/PGC-1α pathway in C57BL/6J male mice. *Food Nutr Res*. **2020**, 64, 3668.

Magnone M, Bruzzone S, Guida L, Damonte G, Millo E, Scarfì S, Usai C, Sturla L, Palombo D, De Flora A, Zocchi E. Abscisic acid released by human monocytes activates monocytes and vascular smooth muscle cell responses involved in atherogenesis. *J Biol Chem*. **2009**, 284, 17808-17818.

Magnone M, Sturla L, Jacchetti E, Scarfì S, Bruzzone S, Usai C, Zocchi E. Autocrine abscisic acid plays a key role in quartz-induced macrophage activation. *FASEB J*. **2012**, 26, 1261-1271.

Magnone M, Ameri P, Salis A, Andraghetti G, Emionite L, Murialdo G, De Flora A, Zocchi E. Microgram amounts of abscisic acid in fruit extracts improve glucose tolerance and reduce insulinemia in rats and in humans. *FASEB J*. **2015**, 29, 4783-4793.

Magnone M, Leoncini G, Vigliarolo T, Emionite L, Sturla L, Zocchi E, Murialdo G. Chronic intake of micrograms of abscisic acid improves glycemia and lipidemia in a human study and in high-glucose fed mice. *Nutrients*. **2018**, 10, 1495.

Magnone M, Emionite L, Guida L, Vigliarolo T, Sturla L, Spinelli S, Buschiazzo A, Marini C, Sambuceti G, De Flora A, Orengo AM, Cossu V, Ferrando S, Barbieri O, Zocchi E. Insulin-independent stimulation of skeletal muscle glucose uptake by low-dose abscisic acid via AMPK activation. *Sci Rep*. **2020**, 10, 1454.

Magnone M, Spinelli S, Begani G, Guida L, Sturla L, Emionite L, Zocchi E. Abscisic acid improves insulin action on glycemia in insulin-deficient mouse models of type 1 diabetes. *Metabolites*. **2022**, 12, 523.

Malik N, Ferreira BI, Hollstein PE, Curtis SD, Trefts E, Weiser Novak S, Yu J, Gilson R, Hellberg K, Fang L, Sheridan A, Hah N, Shadel GS, Manor U, Shaw RJ. Induction of lysosomal and mitochondrial biogenesis by AMPK phosphorylation of FNIP1. *Science*. **2023**, 380, eabj5559.

Michalek RD, Gerriets VA, Nichols AG, Inoue M, Kazmin D, Chang CY, Dwyer MA, Nelson ER, Pollizzi KN, Ilkayeva O, Giguère V, Zuercher WJ, Powell JD, Shinohara ML, McDonnell DP, Rathmell JC. Estrogen-related receptor-α is a metabolic regulator of effector T-cell activation and differentiation. *Proc Natl Acad Sci U S A*. **2011**, 108, 18348-18353.

Mohideen-Abdul K, Tazibt K, Bourguet M, Hazemann I, Lebars I, Takacs M, Cianférani S, Klaholz BP, Moras D, Billas IML. Importance of the sequence-directed DNA shape for specific binding site recognition by the estrogen-related receptor. *Front Endocrinol*. **2017**, 8, 140.

Nemeth E, Ganz T. Regulation of iron metabolism by hepcidin. *Annu Rev Nutr*. **2006**, 26, 323-342.

Oliveira RL, Ueno M, de Souza CT, Pereira-da-Silva M, Gasparetti AL, Bezzera RM, Alberici LC, Vercesi AE, Saad MJ, Velloso LA. Cold-induced PGC-1α expression modulates muscle glucose uptake through an insulin receptor/Akt-independent, AMPK-dependent pathway. *Am J Physiol Endocrinol Metab*. **2004**, 287, E686-E695.

Puce S, Basile G, Bavestrello G, Bruzzone S, Cerrano C, Giovine M, Arillo A, Zocchi E. Abscisic acid signaling through cyclic ADP-ribose in hydroid regeneration. *J Biol Chem*. **2004**, 279, 39783-39788.

Ramzan, R., Vogt, S., & Kadenbach, B. Stress-mediated generation of deleterious ROS in healthy individuals-role of cytochrome c oxidase.*J. Mol. Medicine*, **2020**, *98*, 651-657.

Rangwala SM, Li X, Lindsley L, Wang X, Shaughnessy S, Daniels TG, Szustakowski J, Nirmala NR, Wu Z, Stevenson SC. Estrogen-related receptor alpha is essential for the expression of antioxidant protection genes and mitochondrial function. *Biochem Biophys Res Commun*. **2007**, 357, 231-236.

Rasbach KA, Gupta RK, Ruas JL, Wu J, Naseri E, Estall JL, Spiegelman BM. PGC-1α regulates a HIF2α-dependent switch in skeletal muscle fiber types. *Proc Natl Acad Sci U S A*. **2010**, 107, 21866-21871.

Robinson KM, Janes MS, Pehar M, Monette JS, Ross MF, Hagen TM, Murphy MP, Beckman JS. Selective fluorescent imaging of superoxide in vivo using ethidium-based probes. *Proc Natl Acad Sci U S A*. **2006**, 103, 15038–15043.

Scarfì S, Fresia C, Ferraris C, Bruzzone S, Fruscione F, Usai C, Zocchi E. The plant hormone abscisic acid stimulates the proliferation of human hemopoietic progenitors through the second messenger cyclic ADP-ribose. *Stem Cells*. **2009**, 27, 2469-2477.

Schneider CA, Rasband WS, Eliceiri KW. NIH Image to ImageJ: 25 years of image analysis. *Nat Methods*. **2012**, 9, 671–675.

Schreiber SN, Knutti D, Brogli K, Uhlmann T, Kralli A. The transcriptional coactivator PGC-1 regulates the expression and activity of the orphan nuclear receptor estrogen-related receptor alpha (ERRα). *J Biol Chem*. **2003**, 278, 9013-9018.

Scialò, F., Fernández-Ayala, D. J., & Sanz, A. Role of mitochondrial reverse electron transport in ROS signaling: potential roles in health and disease. *Frontiers in physiology*, **2017**, *8*, 428.

Shin JM, Gwak JW, Kamarajan P, Fenno JC, Rickard AH, Kapila YL. Biomedical applications of nisin. *J Appl Microbiol*. **2016**, 120, 1449-1465.

Sonoda J, Laganière J, Mehl IR, Barish GD, Chong LW, Li X, Scheffler IE, Mock DC, Bataille AR, Robert F, Lee CH, Giguère V, Evans RM. Nuclear receptor ERRα and coactivator PGC-1β are effectors of IFN-γ-induced host defense. *Genes Dev*. **2007**, 21, 1909-1920.

Spinelli S, Begani G, Guida L, Magnone M, Galante D, D'Arrigo C, Scotti C, Iamele L, De Jonge H, Zocchi E, Sturla L. LANCL1 binds abscisic acid and stimulates glucose transport and mitochondrial respiration in muscle cells via the AMPK/PGC-1α/Sirt1 pathway. *Mol Metab*. **2021**, 53, 101263.

Spinelli S, Guida L, Vigliarolo T, Passalacqua M, Begani G, Magnone M, Sturla L, Benzi A, Ameri P, Lazzarini E. The ABA-LANCL1/2 hormone-receptors system protects H9c2 cardiomyocytes from hypoxia-induced mitochondrial injury via an AMPK- and NO-mediated mechanism. *Cells*. **2022**, 11, 2888.

Spinelli S, Cossu V, Passalacqua M, Hansen JB, Guida L, Magnone M, Sambuceti G, Marini C, Sturla L, Zocchi E. The ABA/LANCL1/2 hormone/receptor system controls adipocyte browning and energy expenditure. *Int J Mol Sci*. **2023**, 24, 3489.

Spinelli S, Magnone M, Guida L, Sturla L, Zocchi E. The ABA/LANCL hormone/receptor system in the control of glycemia, of cardiomyocyte energy metabolism, and in neuroprotection: a new ally in the treatment of diabetes mellitus? *Int J Mol Sci*. **2023**, 24, 1199.

Spinelli S, Guida L, Passalacqua M, Magnone M, Cossu V, Sambuceti G, Zocchi E. Abscisic acid and its receptors LANCL1 and LANCL2 control cardiomyocyte mitochondrial function, expression of contractile, cytoskeletal and ion channel proteins and cell proliferation via ERRα. *Antioxidants*. **2023**, 12(9), 1692.

Spinelli S, Guida L, Passalacqua M, Magnone M, Caushi B, Zocchi E, Sturla L. The ABA/LANCL1-2 hormone/receptors system controls ROS production in cardiomyocytes through ERRα. *Biomedicines*. **2024**, 12, 2071.

Spinelli S, Bruschi M, Passalacqua M, Guida L, Magnone M, Sturla L, Zocchi E. Estrogen-related receptor α: a key transcription factor in the regulation of energy metabolism at an organismic level and a target of the ABA/LANCL hormone receptor system. *Int J Mol Sci.* **2024**, 25, 4796.

Spinelli S, Humma Z, Magnone M, Zocchi E, Sturla L. Role of abscisic acid in the whole-body regulation of glucose uptake and metabolism. *Nutrients*. **2024**, 17, 13.

Sturla L, Fresia C, Guida L, Bruzzone S, Scarfì S, Usai C, Fruscione F, Magnone M, Millo E, Basile G, Grozio A, Jacchetti E, Allegretti M, De Flora A, Zocchi E. LANCL2 is necessary for abscisic acid binding and signaling in human granulocytes and in rat insulinoma cells. *J Biol Chem*. **2009**, 284, 28045-28057.

Sturla L, Fresia C, Guida L, Grozio A, Vigliarolo T, Mannino E, Millo E, Bagnasco L, Bruzzone S, De Flora A, Zocchi E. Binding of abscisic acid to human LANCL2. *Biochem Biophys Res Commun*. **2011**, 415, 390-395.

Sturla L, Mannino E, Scarfì S, Bruzzone S, Magnone M, Sociali G, Booz V, Guida L, Vigliarolo T, Fresia C, Emionite L, Buschiazzo A, Marini C, Sambuceti G, De Flora A, Zocchi E. Abscisic acid enhances glucose disposal and induces brown fat activity in adipocytes in vitro and in vivo. *Biochim Biophys Acta Mol Cell Biol Lipids*. **2017**, 1862, 131-144.

Vigliarolo T, Guida L, Millo E, Fresia C, Turco E, De Flora A, Zocchi E. Abscisic acid transport in human erythrocytes. *J Biol Chem*. **2015**, 290, 13042-13052.

Vishwakarma K, Upadhyay N, Kumar N, Yadav G, Singh J, Mishra RK, Kumar V, Verma R, Upadhyay RG, Pandey M, Sharma S. Abscisic acid signaling and abiotic stress tolerance in plants: a review on current knowledge and future prospects. *Front Plant Sci*. **2017**, 8, 161.

Vu EH, Kraus RJ, Mertz JE. Phosphorylation-dependent sumoylation of estrogen-related receptor alpha1. *Biochemistry*. **2007**, 46, 9795-9804.

Wang L, Zou H, Xiao X, Wu H, Zhu Y, Li J, Shen Q. Abscisic acid inhibited reactive oxygen species-mediated endoplasmic reticulum stress by regulating the PPAR-γ signaling pathway in ARDS mice. *Phytother Res*. **2021**, 35, 7027-7038.

Wattez JS, Eury E, Hazen BC, Wade A, Chau S, Ou SC, Russell AP, Cho Y, Kralli A. Loss of skeletal muscle estrogen-related receptors leads to severe exercise intolerance. *Mol Metab*. **2023**, 68, 101670.

Westphal DS, Andres S, Makowski C, Meitinger T, Hoefele J. MAP2 – a candidate gene for epilepsy, developmental delay and behavioral abnormalities in a patient with microdeletion 2q34. *Front Genet*. **2018**, 9, 99.

Zhao HW, Li LJ, Pan J, Han B, Xia H, Wen YM. Apoptosis of Tca8113 squamous cell carcinoma cells induced by abscisic acid in animal models. *Chin J Clin Oncol*. **2008**, 35, 523-526.

Zhou N, Wei Z, Qi Z, Chen L. Abscisic acid-induced autophagy selectively via MAPK/JNK signalling pathway in glioblastoma. *Cell Mol Neurobiol*. **2021**, 41, 813-826.

Zhou N, Yao Y, Ye H, Zhu W, Chen L, Mao Y. Abscisic acid-induced cellular apoptosis and differentiation in glioma via the retinoid acid signaling pathway. *Int J Cancer*. **2016**, 138, 1947-1958.

Zocchi E, Carpaneto A, Cerrano C, Bavestrello G, Giovine M, Bruzzone S, Guida L, Franco L, Usai C. The temperature-signaling cascade in sponges involves a heat-gated cation channel, abscisic acid, and cyclic ADP-ribose. *Proc Natl Acad Sci U S A*. **2001**, 98, 14859-14864.

Zocchi E, Basile G, Cerrano C, Bavestrello G, Giovine M, Bruzzone S, Guida L, Carpaneto A, Magrassi R, Usai C. ABA- and cADPR-mediated effects on respiration and filtration downstream of the temperature-signaling cascade in sponges. *J Cell Sci*. **2003**, 116, 629-636.

Xia, H., Scholtes, C., Dufour, C. R., Ouellet, C., Ghahremani, M., & Giguère, V. Insulin action and resistance are dependent on a GSK3β-FBXW7-ERRα transcriptional axis. *Nature communications*, **2022**, *13*, 2105.

Yan M, Audet-Walsh É, Manteghi S, Dufour CR, Walker B, Baba M, St-Pierre J, Giguère V, Pause A. Chronic AMPK activation via loss of FLCN induces functional beige adipose tissue through PGC-1α/ERRα. *Genes Dev*. **2016**, 30, 1034-1046.

Yoon JC, Puigserver P, Chen G, Donovan J, Wu Z, Rhee J, Adelmant G, Stafford J, Kahn CR, Granner DK, Newgard CB, Spiegelman BM. Control of hepatic gluconeogenesis through the transcriptional coactivator PGC-1. *Nature*. **2001**, 413, 131-138.

Yang X, Liu Q, Li Y, Tang Q, Wu T, Chen L, Pu S, Zhao Y, Zhang G, Huang C, Zhang J, Zhang Z, Huang Y, Zou M, Shi X, Jiang W, Wang R, He J. The diabetes medication canagliflozin promotes mitochondrial remodelling of adipocyte via the AMPK-Sirt1-Pgc-1α signalling pathway. *Adipocyte*. **2020**, 9, 484-494.